

Review

Critical Review on High-Safety Lithium-Ion Batteries Modified by Self-Terminated Oligomers with Hyperbranched Architectures

Debabrata Mohanty ¹, I-Ming Hung ^{1,2,*}, Chien-Te Hsieh ^{1,3,*}, Jing-Pin Pan ⁴ and Wei-Ren Liu ^{5,*}

¹ Department of Chemical Engineering and Materials Science, Yuan Ze University, Taoyuan 32003, Taiwan; debabratamohanty@cgu.edu.tw

² Hierarchical Green-Energy Materials (Hi-GEM) Research Center, National Cheng Kung University, Tainan 70101, Taiwan

³ Department of Mechanical, Aerospace, and Biomedical Engineering, University of Tennessee, Knoxville, TN 37996, USA

⁴ Chief Strategy Office, Far Eastern New Century Corporation, Taipei 10602, Taiwan; jppan@fenc.com

⁵ Department of Chemical Engineering, R&D Center for Membrane Technology, Center for Circular Economy, Chung Yuan Christian University, 200 Chung Pei Road, Chungli District, Taoyuan 32023, Taiwan

* Correspondence: imhung@saturn.yzu.edu.tw (I.-M.H.); cthsieh@saturn.yzu.edu.tw (C.-T.H.); wrliu@cycu.edu.tw (W.-R.L.)

Abstract: In recent years, the evolution of lithium-ion batteries (LIB) has been propelled by the growing demand for energy storage systems that are lightweight, have high energy density, and are long-lasting. This review article examines the use of self-terminated oligomers with hyperbranched architecture (STOBA) as a key electrode additive for the superior performance of LIBs. STOBA has been found to have excellent electrochemical properties, including high specific capacity, low impedance, and good cycling stability when used as an additive in electrode materials. The article discusses the process of synthesis and characterization of STOBA materials, including their potential applications in LIBs as electrode material additives. The article also discusses current research on the optimization of STOBA materials for LIBs, including the use of different solvents, monomers, and initiators. Overall, the review concludes that STOBA materials possess huge potential as a next-generation additive for LIB safety.

Keywords: lithium-ion batteries; high safety; STOBA; self-terminated oligomers; electrode materials



Citation: Mohanty, D.; Hung, I.-M.; Hsieh, C.-T.; Pan, J.-P.; Liu, W.-R. Critical Review on High-Safety Lithium-Ion Batteries Modified by Self-Terminated Oligomers with Hyperbranched Architectures. *Batteries* **2024**, *10*, 65. <https://doi.org/10.3390/batteries10020065>

Academic Editors: Wojciech Mrozik, Vito Di Noto and Wilson K. S. Chiu

Received: 6 December 2023

Revised: 15 January 2024

Accepted: 8 February 2024

Published: 16 February 2024



Copyright: © 2024 by the authors. Licensee MDPI, Basel, Switzerland. This article is an open access article distributed under the terms and conditions of the Creative Commons Attribution (CC BY) license (<https://creativecommons.org/licenses/by/4.0/>).

1. Introduction

1.1. Overview of the Current State of STOBA for Lithium-Ion Battery Technology

Lithium-ion batteries (LIBs) have become an essential technology in a host of utilities from electronics dedicated to consumers to the latest usage in electric vehicles (EVs) [1–3]. The high density of energy and long cycle life of these batteries make them particularly suitable for portable electronics and EVs, where weight is a critical factor, as shown in Figure 1 [4]. In recent years, the evolution of LIBs has been propelled by the growing demand for energy storage systems that are lightweight, have high energy density, and are long-lasting [5,6]. The usage of fossil fuels heightens the need for cleaner and greener energy technologies, such as solar panels, fuel cells, batteries, and wind turbines, and causes a number of environmental and economic problems. The usage of fossil fuels, cars, and other mobile devices is one of the main emitters of greenhouse gases. Accordingly, rechargeable battery systems might be a practical means of achieving the societal aim of switching to an electrified transportation system for the purpose of curtailing emissions. The recent stance on LIB technology is characterized by ongoing research and development to improve performance, safety, and cost. Thus, researchers are working to develop new materials and cell designs that can increase energy density, improve safety, and reduce costs [7,8]. Additionally, the industry is working to improve manufacturing processes to increase production efficiency and reduce costs.

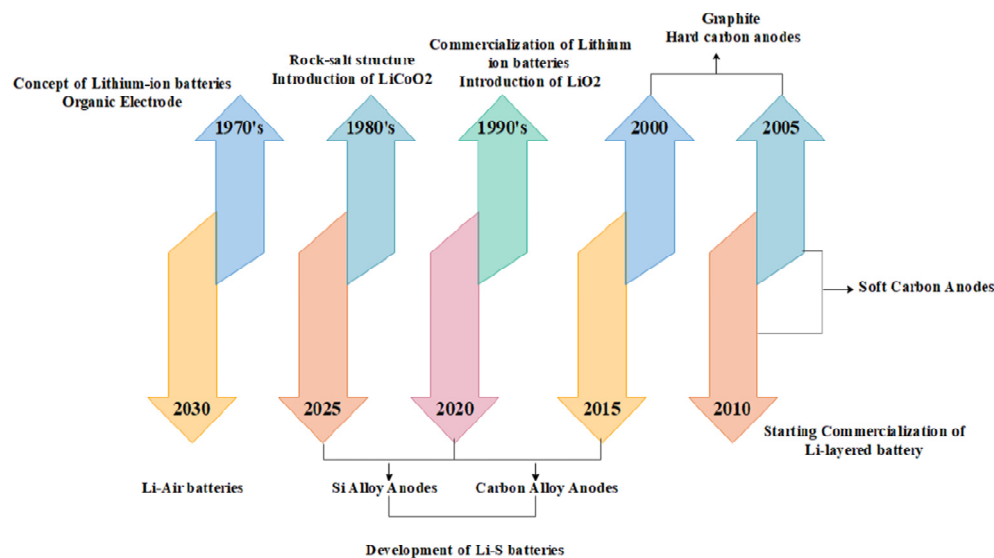


Figure 1. Evolution of lithium-ion batteries [4].

Over the past several decades, numerous battery devices have been developed and made available for purchase. The LIB, extensively utilized in the majority of modern electronics, is presently used in electronic automobiles or hybrid electronic automobiles and is seen as the most successful device in the field of rechargeable battery technology. The growing utility of the in-use batteries inflates safety concerns, and multiple incidents of related mishaps occurring from using LIBs (or packs of them) in EVs and daily electronic gadgets have been documented. Therefore, improving LIB safety is of utmost significance. For instance, mechanical abuse (nail piercing, falling, crushing, vibration, etc.) and electrochemical abuse (short circuits, over-charge and discharge, gas production, etc.), as well as thermal abuse (superficial heating, conflagration assault, hot igniting gases, etc.), may undermine the safety of LIBs [9–12]. The battery might immediately fail due to mechanical abuse, which could result in thermal runaway [13,14]. The emergence of dendrites of lithium on the surface of the negative electrode, dissolved collectors of current, the breakdown of electrolytes alongside gas production and heat initiation, and, lastly, battery thermoelectric instability are all effects of situations involving electrochemical exploitation, such as short circuits, as well as overdischarge/overcharge [15,16]. Additionally, batteries that are heated from the outside may experience thermal runaway more quickly, causing serious damage.

Numerous protective strategies and procedures have been applied both within and outside to help LIBs with their safety issues. “Current interruptive devices (CID)”, “positive temperature coefficient (PTC)” systems, and fuses restraining current, as well as diodes (which can be obstructed or bypassed), are used as external safety methods to reduce possible battery risks under typical operating circumstances [17,18]. Whenever the internal pressure exceeds a certain level, CIDs interrupt the internal electrical connection. To reduce excessive currents, PTC disks are often placed in the cell header. When the temperatures rise quickly, PTC components rapidly increase their resistance and stop the charge conduction at the battery terminal. In situations when a continuous discharge is not preferred, current-limiting fuses might be utilized. Due to sporadic hardware system failures, which generally happen under unusual circumstances, it is currently not feasible to make the LIB 100% secure [19]. Moreover, peripheral components complicate the system and increase the battery pack’s weight, volume, and price, which is unfavorable for batteries consisting of high energy or power densities. Additionally, complicated internal chemistry changes including resistance increases, interfacial phenomena, and current collector corrosion make it difficult for external devices to react quickly [20]. Therefore, it is vitally important to design a trustworthy internal protection system to increase the security of LIBs. To render the battery system risk-proof, advancements to the inside protective workings are

now mostly concentrated upon independent units, together with electrode composites, separators, and electron collectors, as well as electrolytes.

One of the effective internal protection techniques that may be utilized to stop battery overcharging misuse is the redox shuttle. Battery safety may sometimes be increased by using internal protective mechanisms such as shutdown separators, thermosensitive nanostructures, nonflammable electrode compositions, and fire-repelling electrolyte components placed inside negative electrodes or separators [21,22]. Among the misuse scenarios, thermal runaway has drawn a lot of attention due to its detrimental impact on LIB applications. Typical safety issues, particularly with regard to considerable and critical uses, include overcharging, thermic excessive heating, and internal short circuits, which result in thermal runaway. The disintegration along the solid electrolyte interkinetic surface, which results in a significant interlayer decrease well at the lithiated electrode's interface, triggers the thermal runaway mechanism. A sharp temperature rise in thermal runaway is seen when the positive electrode compositions disentangle oxygen, with the oxidization of the electrolytes near the interfaces starting at 180 °C. This can cause the temperature to climb quickly, reaching several hundred degrees in a matter of seconds.

Recent advances in LIB technology include the evolution of current cathode materials, like “nickel cobalt manganese oxide (NCM)”, which have higher energy densities than traditional cathode materials [23,24], as well as anode materials, such as silicon and lithium–sulfur, that have the potential to significantly increase energy density [25]. Furthermore, the development of solid-state batteries, which utilize solid electrolytes in place of liquid electrolytes, is expected to significantly increase safety [26]. However, despite these advances, there are still significant challenges facing the LIB industry. One major challenge is cost, as LIBs are still relatively expensive compared to other forms of energy storage devices [27]. Additionally, the recycling of disposal LIBs is a significant concern, as these batteries contain toxic materials that can be harmful to the environment if not properly handled [28]. In conclusion, the current state of LIB technology is characterized by ongoing research and development to improve performance, safety, and cost. Researchers are working to develop new materials and cell designs that can increase energy density, improve safety, and reduce costs. Moreover, the industry is working to improve manufacturing processes to increase production efficiency and reduce costs. While there are still significant challenges facing the LIB industry, the future of this technology looks promising as researchers continue to make advances in design and manufacturing processes.

LIBs have become an essential technology for a variety of works, from consumer-based electronics to EVs. However, the use of these batteries is not without challenges. One of the main challenges facing the LIB industry is the evolution of the latest materials that can improve performance, safety, and cost. One promising area of research is the use of self-terminated oligomers with hyperbranched architecture (STOBA) in LIBs [29]. The Industrial Technology Research Institute (ITRI, Taiwan) has created a series of STOBA materials that may be layered over positive electrodes to minimize the danger of thermic control in an effort to tackle the thermal runaway issue [30]. STOBA as a novel additive material can be used to optimize the battery properties in the electrochemical, as well as thermal runaway, aspect. According to the research by Lin et al., the STOBA coating significantly decreased thermal runaway despite having a noteworthy impact on the electrochemical performance of LIBs. The STOBA layering effectively prevented the heat from increasing quickly, as demonstrated by the nail penetration test [31]. In less than two seconds, the temperature of a cell with a $\text{Li}(\text{Ni}_{0.4}\text{Co}_{0.2}\text{Mn}_{0.4})\text{O}_2$ cathode even with no STOBA plating rose to almost 700 °C. Furthermore, unintentional internal or external short circuits may be the root of a cell's fast heat creation [32]. A thorough investigation has not yet been conducted to examine the function of the STOBA interlayer in inhibiting circuit breakdowns, as well as, consequently, the thermal controls of an energy storage system. In this work, the changes in the structure of the STOBA layer at various temperatures, as well as the STOBA–cathode interface in the completely charged state, were examined in order to better understand the safety mechanism.

1.2. Background and Motivation for the Use of STOBA Materials in LIBs

STOBA materials are a class of polymeric materials that have been found to have several advantages over traditional LIB materials [32]. These materials have a unique branched architecture, which allows for a higher degree of flexibility and adaptability in the design of the polymer. Figure 2 shows the self-terminated nature of the oligomers in STOBA that allow for more control over the properties and structure of the polymer as it is heated [32–34]. The use of STOBA materials in LIBs has several potential advantages. For example, these materials can be used to create more stable and reliable LIBs. Additionally, the unique properties of these materials may make it possible to create batteries with higher energy densities, longer cycle lives, and improved safety [35,36]. The background and motivation for the utilization of STOBA materials in LIBs can be attributed to the search for new materials that can enhance the safety and performance of these batteries. The unique structure and properties of STOBA materials make them a promising candidate for use in LIBs. Furthermore, the use of STOBA compositions has the potential to convey the current challenges facing the LIB industry and open new possibilities for the development of high-performance and safe LIBs. In this article, we will lay out the background and motivation for the use of STOBA materials in LIBs, including an examination of the unique properties of these materials and their potential advantages for use in LIBs. Furthermore, we will discuss the current state of research on STOBA materials in LIBs and important challenges that still need to be addressed.

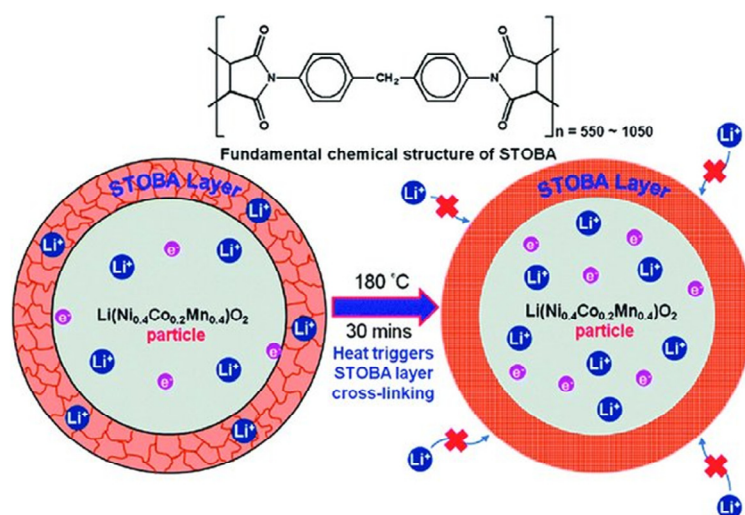


Figure 2. Scheme of morphology change of the STOBA coating in the STOBA-coated $\text{Li}(\text{Ni}_{0.4}\text{Co}_{0.2}\text{Mn}_{0.4})\text{O}_2$ cathode before and after heating [32].

Thus, STOBA has amassed recognition in the current decade given its unique properties and potential applications in diverse fields including electronics and medicine, along with material research. The use of various techniques, solvents, monomers, and initiators. This review focuses on the different fabrication techniques for STOBA materials, including the addition of different solvents, monomers, and initiators. We will also review the recent advancements in the field and the challenges that still need to be addressed for the successful synthesis of these materials, as well as their thermal and electrochemical advancement. Overall, this article focuses on providing a comprehensive outline of such directional advancements in STOBA synthesis, as well as highlighting the potential of these materials in numerous applications. In particular, STOBA materials were researched for their potential use as electrolytes for LIBs. The synthesis of STOBA materials is a complex process that involves the use of various techniques, solvents, monomers, and initiators. In this article, we will discuss the different methods for the synthesis of STOBA materials, including the applications in different solvents, monomers, and initiators, with a specific focus on their utilization in LIBs.

2. Synthesis and Characterization of STOBA Materials

2.1. Synthesis of STOBA Materials: Effect of Solvents, Monomers, and Initiators

One of the key challenges in the synthesis of STOBA materials is achieving the desired level of branching and control over the molecular weight [37]. One common method for achieving this is the “living” or “controlled” polymerization approaches, namely, the “atom transfer radical polymerization (ATRP)” or “reversible addition–fragmentation chain-transfer (RAFT)” polymerization. These methods allow for the exact regulation of the molecular mass, as well as the branching of the polymer, which is essential in the development of powerful electrolytes [38].

The other crucial factor in lieu of synthesis of STOBA materials is the choice of solvent. The selection of a solvent plays a pivotal role in the polymerization process and can affect the properties of the resulting materials. Common solvents used in the synthesis of STOBA materials include “dimethyl sulfoxide (DMSO), tetrahydrofuran (THF), and *N,N'*-dimethylformamide (DMF)” [39]. These solvents are polar and have a high dielectric constant, which allows for efficient charge transfer and improved conductivity in the resulting materials. In contrast, 4-(2,4-Dichlorophenoxy) butyric acid is a nonpolar compound, and as such, it is best dissolved in a nonpolar solvent [40]. The solvent dichloromethane (DCM) is a commonly used solvent for STOBA due to its nonpolar properties and high solubility for nonpolar compounds. However, DCM is toxic and can be harmful if inhaled or ingested, so appropriate precautions must be taken when using this solvent. Toluene is another commonly used solvent for STOBA due to its high solubility for nonpolar compounds and low toxicity compared to DCM. However, it is flammable and must be handled with care. Hexane is a highly nonpolar solvent that is often used for dissolving STOBA. Although hexane possesses high solubility for nonpolar compounds and low toxicity, it is also flammable and must be handled with care. Chloroform is a polar solvent that is sometimes used to dissolve STOBA. Although it has a higher solubility for polar compounds, its polar nature may result in decreased solubility for nonpolar compounds like STOBA. Additionally, chloroform is toxic and should be handled with caution. Acetone is a highly polar solvent that is not commonly used for dissolving STOBA due to its low solubility for nonpolar compounds. It is also highly flammable and should be handled with caution. Accordingly, the choice of solvent for dissolving STOBA will depend on various factors, namely, solubility, compatibility with other materials in the system, and toxicity/flammability of the solvent. It is always best to consult a specialist or reference a reliable source before selecting a solvent for a specific application.

Excellent mechanical qualities, chemical resistance, and thermal stability are provided by the polyimides that result from the reaction of *N,N'*-bismaleimide-4,4'-diphenylmethane (BMI) with barbituric acid (BTA), which display hyperbranched or strongly conjoined matrix architectures [41]. As a result, these items have seen extensive use in sectors including electronics and aerospace. Thus, BTA was shown to start the independent radical polymerizations of BMI or bisphenol A diglycidyl ether diacrylate in prior investigations. Furthermore, the group of BMI, $-C=C-$, could react with BTA, which imparts two $-NH$ groups, as well as one $-CH_2$ group, via the aza-Michael addition and Michael addition reaction mechanisms, respectively. However, in the polymerizations of BMI with BTA, competitive free radical and Michael addition polymerizations were more common. It is also noteworthy to observe that the two $-NH$ groups of BTA or 5,5'-dimethylbarbituric acid (55BTA) have little reactivity with the $-C=C-$ group of BMI. Contrarily, the hyperbranched polymer produced when BMI was combined with cyanuric acid (CA, which has three $-NH$ groups) and triethylamine (TEA), functioning as a primary catalyst for the aza-Michael addition reaction, was exclusively produced by the aza-Michael addition reaction mechanism (as shown in Figure 3) [42]. Herein, STOBA, a special type of polymer created by polymerizing BMI with BTA, has been utilized as a supplement to give LIBs many protection layers against thermal runaway and eventually catastrophic explosion. In addition, as indicated previously, the aza-Michael addition reaction mechanism played a major role in controlling the reaction of BMI with CA in the presence of TEA that produced polymers

with a hyperbranched structure. Investigations into the self-polymerization of heat and radical polymerization, as well as polymerization with diamine, polyamine, ethyl alcohol, and diphenol, have been conducted using *N,N'*-bismaleimide-4,4'-diphenylmethane (MDA-BMI). The tautomerization characteristics and resonance structures of calculations involving the BTA molecule have received the majority of attention in these studies.

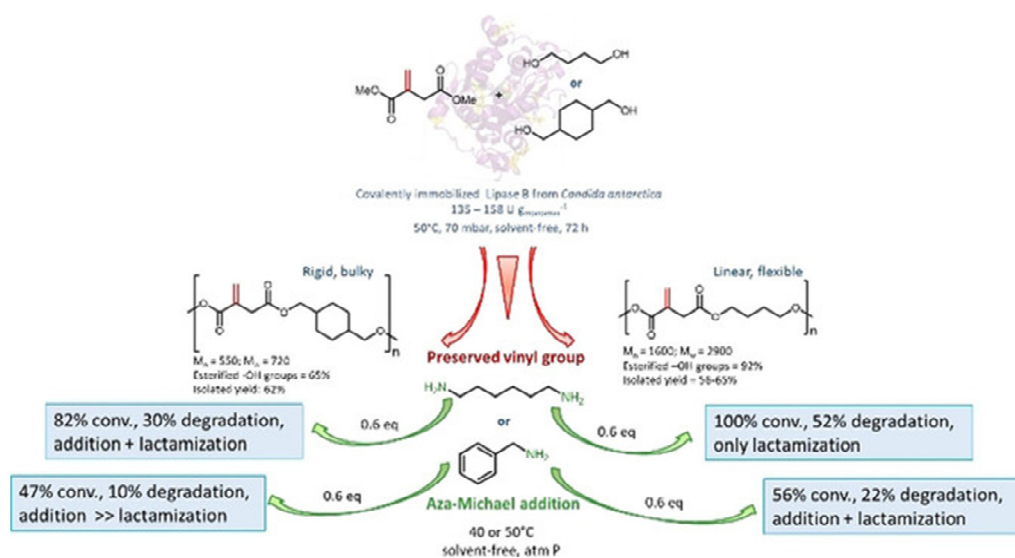


Figure 3. Functionalization of enzymatically synthesized rigid poly(itaconate)s via post-polymerization aza-Michael addition of primary amines [42].

Generally, STOBA is a type of branched polymer that can be synthesized by a controlled polymerization process. The common methods used for the synthesis of STOBA materials can be described as follows. The living anionic polymerization method involves the use of a strong base to initiate the polymerization reaction [43], followed by the inclusion of a chain-transfer factor to control the polymerization process and limit the length of the polymer chains. The end result is a branched polymer with a well-defined molecular weight dispersal and an abundance of branching. ATRP is administered by the radical polymerization method that is based on the movement of a halide to a transition metal complex [44]. In the presence of a chain-transfer agent, the growth of the polymer chains is limited, resulting in a branched polymer with a well-defined molecular weight distribution and a high degree of branching. In contrast, RAFT polymerization is another controlled radical polymerization method that is based on the use of a chain-transfer agent [45]. The chain-transfer agent acts as both an initiator and a controller of the polymerization process, resulting in a branched polymer with a well-defined molecular weight distribution and a high degree of branching. Ring-opening metathesis polymerization (ROMP) is a metathesis polymerization method that involves the ring-opening of cycloolefins by a metathesis catalyst [46]. By controlling the monomer feed and the reaction conditions, it is possible to synthesize branched polymers with a well-defined molecular weight distribution and a high degree of branching. The controlled/living cationic polymerization method involves the use of a Lewis acid to initiate the polymerization reaction, followed by the inclusion of a chain-transfer factor to control the polymerization process and limit the length of the polymer chains. The end result is a branched polymer with a well-defined molecular weight distribution and a vehemence of branching. There are several methods available for the synthesis of STOBA materials, each illuminating their own advantages and impediments. The adoption of techniques is influenced by variables like the intended molecular weight dispersal, the amount of branching, and the compatibility with other materials in the system. It is always best to consult a specialist or reference a reliable source before selecting a synthesis method for a specific application.

The choice of monomer and initiator will affect the properties of the resulting STOBA material, including its molecular weight dispersal, intent of branching, and solubility. The monomers used in the synthesis of STOBA materials can vary widely depending on the desired properties of the final products. Common types of monomers used for the synthesis of STOBA materials include acrylates, methacrylates, and vinyl esters. The choice of initiator will affect the rate of polymerization and the molecular weight distribution of the final STOBA material. Common initiators used in the polymerization process include copper (II) chloride and benzyltrimethylammonium chloride, while common monomers include cyclic oxide and ethylene oxide [47]. These monomers have been shown to have good solubility in common solvents, which helps to improve the conductivity of the resulting materials. Common types of initiators used for the synthesis of STOBA materials include strong bases for anionic polymerization, Lewis acids for cationic polymerization, and radical initiators for radical polymerization [48]. Chain-transfer agents are used in the synthesis of STOBA materials to control the polymerization process and limit the length of the polymer chains. Common types of chain-transfer agents include mercaptans for radical polymerization, thiols for anionic polymerization, and Lewis acids for cationic polymerization. The polymerization conditions, such as temperature, pressure, and the presence of a solvent, will also affect the properties of the final STOBA material. It is important to carefully control these conditions to ensure the desired molecular weight distribution and branching intensity, as well as solubility, of the final product. The choice of monomer, initiator, and polymerization conditions will play an essential role in determining the properties of the final STOBA material.

2.2. Characterization Techniques for STOBA Materials

Once the STOBA materials have been synthesized, it is crucial to evaluate their properties and performances in order to assess their suitability for use in LIBs. Common methods for evaluating the properties of STOBA materials include thermal analysis techniques such as differential scanning calorimetry (DSC) and thermogravimetric analysis (TGA), as well as electrochemical methods like cyclic voltammetry (CV) and electrochemical impedance spectroscopy (EIS). Recent studies have shown that STOBA materials have good thermal stability, high conductivity, and low viscosity, which make them promising candidates for use as electrolytes in LIBs [49]. Even so, there are challenges, waiting to be found, to achieve the required level of performance. For example, the low thermal stability of some STOBA materials can be a constraint to their utility in high-temperature applications. Additionally, the development of methods for the synthesis of STOBA materials obtaining the optimal molecular weight, as well as a high intensity of branching, is still an area of active research. As such, to fully acknowledge the properties and behavior of these materials, it is essential to use various characterization techniques to study them. This critical review focuses on different characterizations for STOBA materials, including Fourier transform infrared (FTIR) spectroscopy, nuclear magnetic resonance (NMR), and transmission electron microscopy (TEM). FTIR is a common technique used to study the chemical structure of STOBA materials [50]. This technique is based on the absorption of infrared radiation by a material, and it can provide information on the functional groups present in the material, as well as the chemical bonding. FTIR can be utilized to detect the existence of functional groups such as ethers, esters, and amides, which are commonly found in STOBA materials. Additionally, FTIR can be exercised to characterize the thermal stability of STOBA materials, as the absorption spectrum can be obtained at different temperatures. NMR is another powerful technique that can be used to examine the chemical structure of STOBA materials. NMR is based on the principle that the nuclei of certain atoms, such as hydrogen and carbon, have a magnetic moment that can be manipulated by an external magnetic field. NMR can be used to calculate the number and various categories of atoms present in a material, as well as their chemical environment. Additionally, NMR can also be employed to investigate the molecular dynamics of STOBA materials, as it can provide information on the mobility and interactions of the atoms within the material. TEM is a technique that can

be used to study the microstructure of STOBA materials. TEM is based on the transmission of electrons through a thin sample, and it can render direction about the distribution shape, as well as size factors, of particles within the compound. Additionally, TEM can also be used to study the morphology of STOBA materials, as it can provide information on the structure and organization of the particles within the material. In addition to these techniques, other characterization methods, namely, X-ray diffraction (XRD), scanning electron microscopy (SEM), and dynamic mechanical analysis (DMA), can be exploited to study STOBA materials [51,52]. XRD can be used to explore the crystal structure along with the crystallinity of the materials, SEM can be used to study the surface morphology, and DMA can be applied to study the hardness properties of the samples. Overall, the characterization of the STOBA compound is of utmost importance to fully understand the properties and behavior of these materials. The combination of different characterization techniques, such as FTIR, NMR, and TEM, can provide a comprehensive analysis of the materials, enabling researchers to better understand the structure–property relationships of the materials. Furthermore, understanding the properties of these materials is important for rational design, as well as the development of advanced compounds with upgraded characteristics and functionality.

3. Electrochemical Properties of STOBA Materials

3.1. Effect of STOBA Additive on Specific Capacity, Impedance, and Cycling Stability

STOBA materials have recently gained attention as potential additives for electrode materials, citing their unique electrochemical properties. In this article, we will discuss the specific capacity, impedance, and cycling stability of STOBA materials on other anodes in LIBs. Specific capacity is a measurement of the amount of energy that a substance can hold per mass unit, which also depends on the thermal management of the batteries. Figure 4 [53] depicts the different stages of the thermal runaway of LIBs. This occurs due to the unique structure of the materials, which allows for more lithium ions to be stored in the electrode materials. The impedance of a material is affected by its composition, structure, and electrochemical properties. STOBA materials have been found to exhibit low impedance values, indicating their ability to facilitate the flow of electrical current. This property is highly advantageous for enhancing the electrochemical performance of LIBs as it enables faster charging and discharging. In addition, cycling stability is essential to the effectiveness of LIBs, as it determines how well a material can maintain its capacity and impedance over repeated charge and discharge cycles. STOBA addition in electrode materials has demonstrated excellent cycling stability, which is essential for the longevity of LIBs. Compared to other anode material additives, STOBA materials offer several advantages, including higher specific capacity, lower impedance, and better cycling stability. These properties make them promising candidates for the creation of LIB electrode components with higher efficiency with the required safety.

3.2. Explanation of How STOBA Materials Contribute to Electrochemical Properties

The unique structure of STOBA materials is a result of the self-termination reaction of the oligomers during synthesis. This results in a highly branched, three-dimensional structure with a large surface area. This hyperbranched structure provides several advantages for electrolytes. One of the main advantages of the hyperbranched structure is the increased specific capacity. As shown in Figure 5 [54], the large surface area allows for more lithium ions to be stored in the material, resulting in a higher specific capacity. This means that STOBA materials can store more energy per unit mass than other anode materials. The hyperbranched structure also improves the cycling stability of STOBA materials. The large number of branches provides multiple pathways for lithium ions to move through the material during charging and discharging. The hyperbranched structure also contributes to the low impedance of STOBA materials. The branches provide multiple pathways for electrical current to flow through, which reduces the resistance to current flow. This improves the rate performance of the STOBA-added anode and allows for fast charge/discharge. In

In addition to the electrochemical properties, the hyperbranched structure also contributes to the mechanical stability of STOBA materials. The branches act as a buffer against volumetric changes during charging and discharging, which improves the stability of the material and reduces the formation of cracks and defects. Therefore, the hyperbranched structure of STOBA materials is a key factor in their excellent electrochemical properties. The large surface area, multiple pathways for lithium-ion movement, and low resistance to current flow all contribute to the high specific capacity, excellent cycling stability, and low impedance of STOBA materials. These properties make them a favorable anode material for LIBs. However, further research is needed to fully understand their properties and to develop ways to scale up their production.

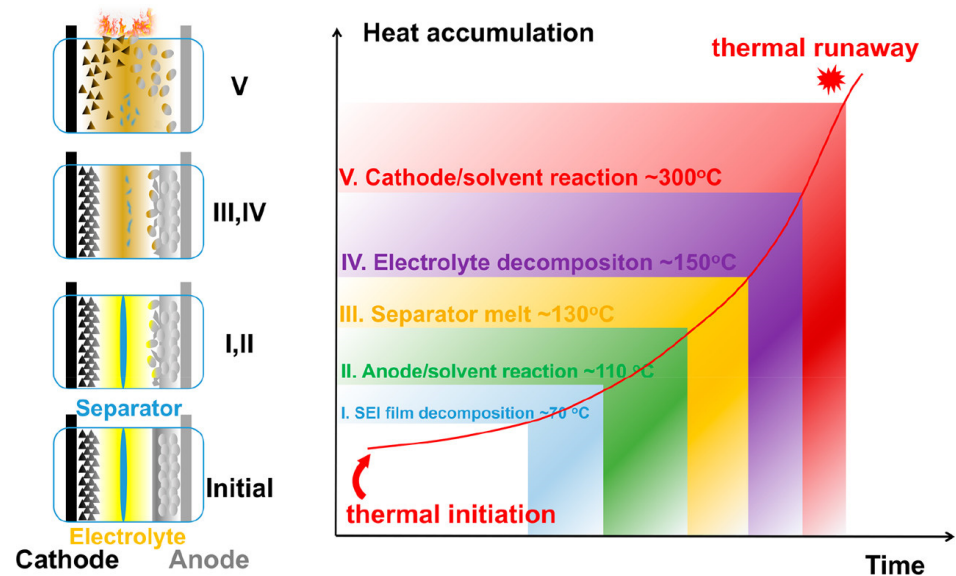


Figure 4. Schematic of the classification of thermal runaway stages of LIBs [53].

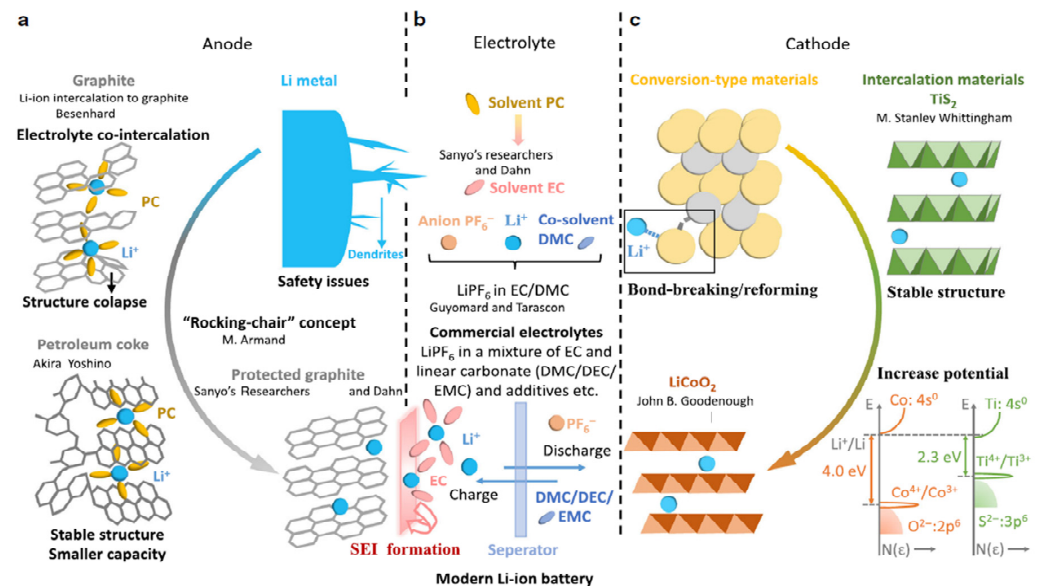


Figure 5. Milestone discoveries that shaped the modern lithium-ion batteries. The development of (a) anode materials including lithium metal, petroleum coke, and graphite, (b) electrolytes with the solvent propylene carbonate (PC), a mixture of ethylene carbonate (EC), and at least one linear carbonate selected from dimethyl carbonate (DMC), diethyl carbonate (DEC), ethyl methyl carbonate (EMC), and many additives, (c) cathode materials including conversion-type materials, intercalation materials titanium disulfide (TiS_2), and lithium cobalt oxide (LiCoO_2) [54].

4. Applications of STOBA Materials in LIBs

4.1. Portable Electronics, EVs, and Renewable Energy Storage Systems

One of the main potential applications of STOBA materials is in portable electronics [55]. LIBs are commonly used in portable electronics such as smartphones, laptops, and tablets given their high energy density and long-lasting performance. The high specified capacity and excellent cycling stability of STOBA materials make them well suited for use in portable electronics, as they can provide longer battery life and more power in a smaller package. STOBA materials also have potential in EVs [56]. The high specific capacity and low impedance of STOBA materials can improve the range and performance of EVs. Additionally, the excellent cycling stability of STOBA materials can extend the life of the battery, which is critical for the high-use scenario of EVs. Another potential application of STOBA materials is in renewable energy storage systems. With the increasing use of green sources of energy including solar and wind power, effective energy retention systems are needed to store the energy generated when it is not being used. The optimal specific capacity and minimal impedance, along with the excellent cycling stability of STOBA materials make them well suited for use in renewable energy storage systems, as they can provide long-lasting and efficient storage of renewable energy. Furthermore, STOBA materials have a huge range of potential applications in LIBs, including electric cars, portable gadgets, and sustainable systems for storing energy. The unique properties of STOBA materials, such as high specific capacity, low impedance, and optimum cycling stability, make them well suited for these applications [57]. However, further research is needed to fully understand their properties and to develop ways to scale up their production.

4.2. Optimization of STOBA Materials for LIBs

STOBA materials have a high specific capacity, which is a standard of how much energy a material can store per unit mass. This means that they can store more energy per unit mass than other anode material additives, which is beneficial for LIBs. The enhanced specific capacity from STOBA materials is due to their unique hyperbranched structure, which allows for more lithium ions to be stored in the material. STOBA materials also have a low impedance, which is a measure of how easily electrical current flows through a material. This means that electrical current can flow through STOBA materials easily, which is beneficial for LIBs, and enables the battery to charge and discharge quickly. Materials with STOBA also have excellent cycling stability, which is a measure of how well a material can maintain its performance over multiple charge and discharge cycles. This reveals that they can maintain their high specific capacity and low impedance over many charge and discharge cycles, which is important for LIBs. The unique hyperbranched structure of STOBA materials also contributes to the mechanical stability of the material, which is paramount to the sustainable performance and longevity of the battery. Furthermore, current research is aimed at improving the synthesis methods of STOBA materials, increasing their specific capacity, improving their cycling stability, and reducing the cost of the materials. This will lead to a more practical and cost-effective application in various disciplines like electric cars, portable gadgets, and sustainable systems for storing energy.

Carbonaceous materials, namely, graphite, are customarily in usage as anode materials in rechargeable LIBs studied by Hwang et al. [58]. “LiCoO₂ is the primary material used as the positive electrode in present-day commercial LIBs given its record theoretical capacity, working potential, and magnificent cycling ability at room temperature. But one major challenge in utilizing these electrodes is the marked oxidative decomposition of the electrolytes on the electrode surface, which results in high capacity loss and poor cycling ability.” To address this issue, several additives have been used to modify the solid electrolyte interface (SEI) layer over the electrode interface, as seen in Figure 6 [59]. These additives should be reduced or oxidized before being introduced into the electrolyte to prevent further decomposition of the SEI layer. While some additives can improve battery safety, they may negatively affect battery performance, and an additive that has a positive effect on the anode may show negative effects on the cathode.

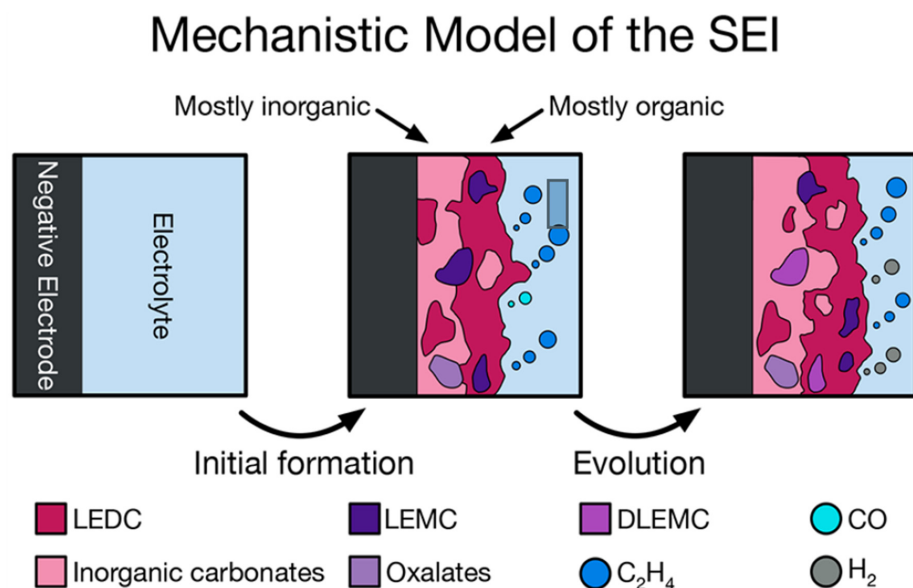


Figure 6. Mechanistic model of solid–electrolyte interphase formation [59].

Silicon polymers are a versatile cluster of materials that have been widely used in various applications due to their human friendliness and universal properties studied by Plichita et al. [60]. 3-aminopropyl trialkoxysilane is a silicon-based chemical compound that is commonly used in industrial processes that produce siloxane compounds, silica nanoparticle compounds, or silane-containing particulates. The goal of this study was to synthesize branched oligomers established on trialkoxysilane under different conditions, as well as further apply them to alter urethane prepolymer. To achieve this, as shown in Figure 7 [60], the primary amino group of APTES was reacted with a five-membered EC to obtain a hydroxyl-terminated alkoxy silane monomer and oligomers. The ideal circumstances for synthesizing APTES-OH monomers with high precision were found to be a reaction at a temperature of 20–25 °C instead of utilizing a catalytic agent. Meanwhile, to obtain the APTES-OH oligomers with maximum effectiveness, the process must be sustained at a high enough temperature using a catalyst, preferably based on Ti.

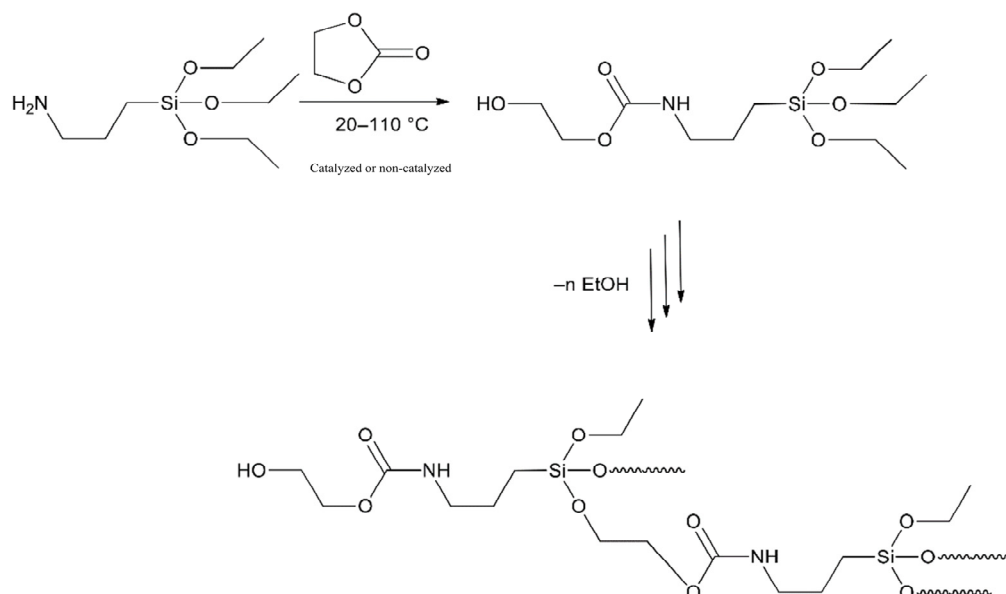


Figure 7. Scheme of the synthesis of APTES-OH monomer and its (hyper)branched oligomers terminated with a hydroxyl group [60].

Feng et al. [61] explored the application of the accelerating rate calorimetry (ARC) technique to evaluate the thermal runaway (TR) features of battery cells. Different ARC models were used for testing small and large format samples. The ARC curves were analyzed together with differential scanning calorimetry (DSC) results for the constituent substances to gain insights into the heat generation mechanisms of the battery cells. The Hatchard model, evolved on the principle of thermodynamic overlaying, was employed to interpret the mixed reactions in the system, the results of which can be seen in Figure 8 [61]. By comparing the ARC outcomes for cells and the DSC results for the electrodes, it was found that the exothermic reactions within the $\text{SYS}_{\text{AN}}^{\text{ELE}}$ component were the primary thermal source of devices with NMC or LFP cathodes. The thermal review database developed at Tsinghua University provided a useful resource for studying the current lithium-ion devices' highly exothermic mechanics, and it revealed that for systems with something like a LiO_2 electrode, the primary source of heat throughout heat dissipation was indeed the redox interaction seen between the anode and cathode.

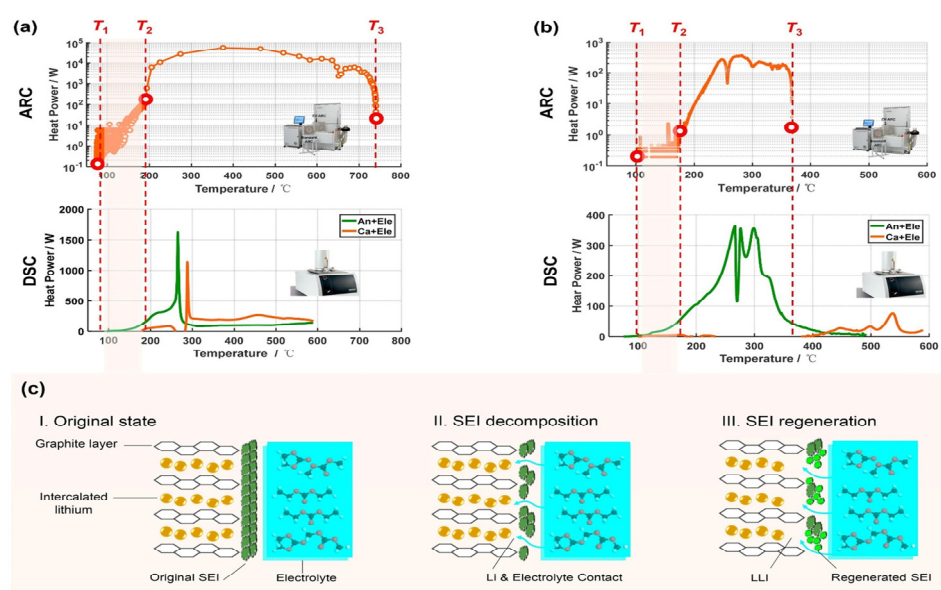


Figure 8. Interpretation of the heat generation mechanisms between T_1 and T_2 . (a) Comparison of the total heat generation power results from the ARC and DSC tests, for Cell Type A, with an NCM + LMO cathode and an MAG10 anode. (b) Comparison of the total heat generation power results from ARC and DSC tests, for Cell Type F, with an LFP cathode and an MCMB anode. (c) Mechanism of heat generation between T_1 and T_2 [61].

To ensure battery safety, protection mechanisms can be external or internal, which was described by Liu et al. [62]. The latter approach employs per se safe materials for components of the battery, making it the “ultimate” solution for battery safety. Recent developments in material design have produced progress in resolving battery safety issues. Flammable substances that can put out crystalline lattice fires are strongly sought to improve battery protection. Polymer binders or conductive frameworks that contain flammable substances can be combined with graphite. While ongoing reviews concentrate on the materials' ground safety, a whole-person strategy to address the flammability of LIBs ought to be considered. Ingredients, cell layout and constituents, battery modules, and modules all have similar importance in ensuring batteries are dependable before being offered for sale.

According to Kao et al. [63], the addition of external devices to a battery system results in increased complexity, weight, volume, and costs, which are not conducive to high-energy or power-dense batteries. While thermal runaway is a concern for LIBs, a detailed analysis of how the solid-state electrolyte (SSE) layer restricts short circuits and, consequently, thermal runaway has not been conducted. Therefore, Kao et al. conducted

nitrogen adsorption–desorption measurements to examine the SSE’s porous architecture in the material, STOBA, under different thermic experimental conditions. It has been found that the thermal runaway of LIBs occurs above 180 °C due to the emission of O₂, as well as the heat from the reaction of the electrode material, leading to the interfacial oxidation of the electrolyte and expedited increase in temperature. Nitrogen adsorption–desorption quantification revealed that the porosity of STOBA disappears at around 180 °C, which suggests that the chains in STOBA crosslink with one another and then melt at high temperatures. Furthermore, Kao et al. observed changes in the STOBA chains through nitrogen adsorption–desorption measurements and SEM (see Figure 9) [63]. These changes indicate that the chains in STOBA crosslink with one another and lead to an elevated degree of crosslinking with rising temperatures, resulting in the transformation of the STOBA interlayer changing from porous to nonporous.

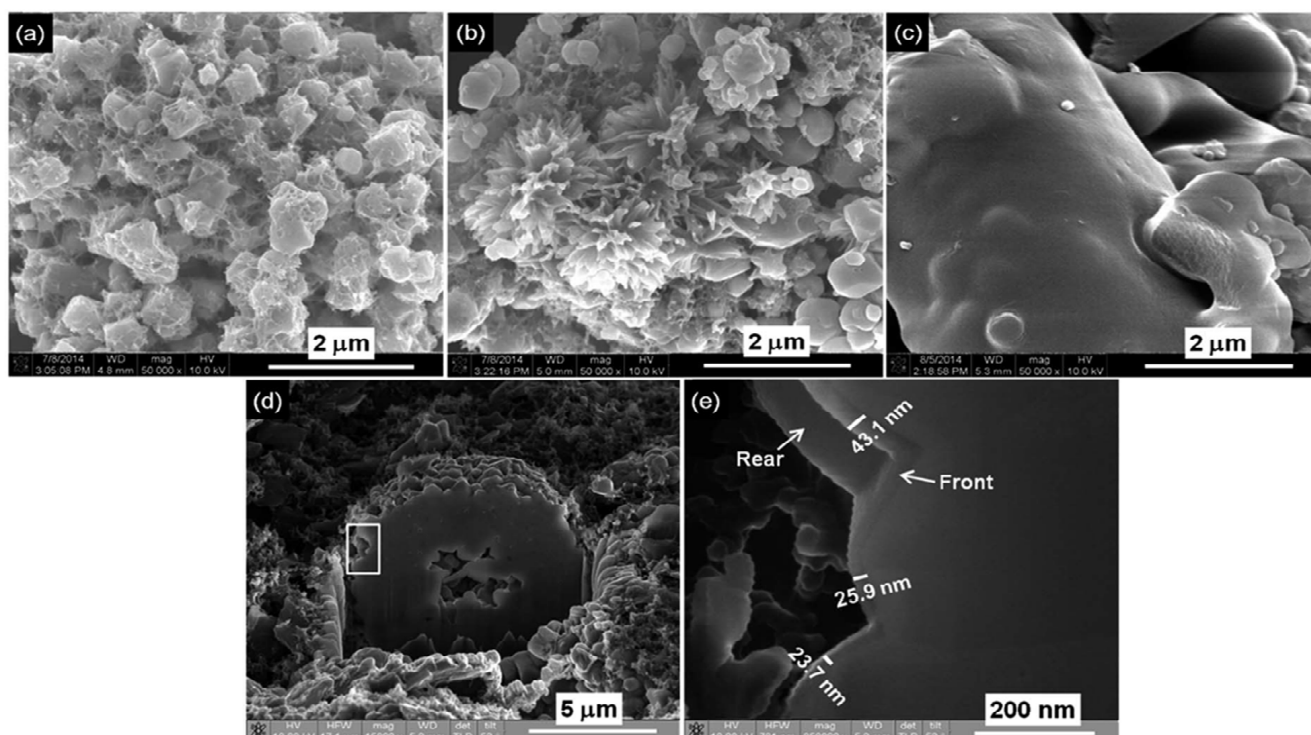


Figure 9. SEM images of STOBA material (a) without thermal treatment and with thermal treatment at (b) 150 °C and (c) 180 °C, and (d) cross-section of a STOBA-coated $\text{Li}(\text{Ni}_{0.4}\text{Co}_{0.2}\text{Mn}_{0.4})\text{O}_2$ particle. The marked region of (d) is shown as an enlarged image to (e) illustrate the STOBA coating thickness on the $\text{Li}(\text{Ni}_{0.4}\text{Co}_{0.2}\text{Mn}_{0.4})\text{O}_2$ particle [63].

In their research, Duh et al. [64] discussed the hazards in relation to thermal runaway and incidents related to LIBs. They provided a list of transnational fire incidents caused by various types of LIBs due to failures. The number of fire incidents caused by LIBs has increased significantly since 2016, coinciding with the surge in demand for smartphones and EVs. To assess the thermal runaway hazards of 18,650 LIBs, the researchers selected six parameters: T_{Onset} , T_{cr} , T_{max} , P_{max} , Δn , and ΔH . It was found that the 18,650 LFP battery is safer than other batteries under abusive scenarios. For non-LFP batteries, a T_{cr} of 200 °C and a maximum rate of 100 °C min^{-1} were chosen to evaluate the no-return hazard and rate hazard. While the safety of batteries at the level of material is what the research focuses on, it really is crucial to follow a holistic function that considers the safety of cell components and layout, as well as battery modems with packs, to produce batteries that are more reliable before releasing them to the public.

Pham et al. [65] studied the synthesis of polymers with hyperbranched structures for the advancement of LIBs. They reported that *N,N'*-bismaleimide-4,4'-diphenylmethane reacted with cyanuric acid (CA) in accordance with trimethylamine via aza-Michael addition reaction to form hyperbranched BMI/CA polymers that advanced battery performance. Another type of polymer was obtained by reacting BMI with 55BTA (barbituric acid) in the presence of Ph₃P, which could also be a good addition to LIBs. The authors investigated the dynamics and processes involved in the polymerization of BMI with 55BTA in accordance with Ph₃P, using approaches to estimate the energy barrier using both prototype and framework techniques, pre-exponential factor, and reaction modeling. The results showed that linear polymers could be derived from the polymerization of BMI, along with 55BTA, in the presence of Ph₃P and hydroquinone at temperatures between 40 and 90 °C, while hyperbranched polymers could be synthesized in a broad temperature range of 60–150 °C.

Deruelle et al. [66] extracted the percent signal change with regard to the three approaches in the active cluster and a right hemispheric reflecting ensemble. The rmANOVA analysis indicated that the grouping and agent had meaningful contact, suggesting that the hypothalamic activity's lateralization in the tight standards led to a brain-wide assessment utilized in place of functional lateralization. In the analysis of activity, the left PHN complex in terms of capability was linked to a solitary cluster at the left temporoparietal intersection, which is in contradiction to the hypothalamic complex in terms of interaction. A study reported the beneficial effects of a lack of anthropomorphism on how young autistic children perceive animals' motion. When controls played against a robot, running against people caused a noticeably worse ITPJ/PHN communication, indicating a similar effect. The results hint that within the general population, signals regarding the social environment and hypothalamic chemicals, including oxytocin, influence the pleasant rewards from social engagement, linked to the left temporoparietal intersection.

In a previous study by Pan et al., it was shown that a branched oligomer with oxidative SEI elevates the performance of a self-polymerized membrane and provides very good heat and high-temperature durability. In an insightful work by Li et al. [67], the same branched oligomer (BO) was selected as an additive to improve the electrochemical performance of lithium-ion cells. The impact of various BO contents on cellular functioning was investigated. The 503759-type full cell cycle performance was evaluated at a charge–discharge rate of 0.5 C at ambient temperature. The results of Figure 10 [67] showed that the cycle performance of the cells with 1.0 wt% BO additive was superior compared to those without the additive and those with 2.5 wt% additive for 400 cycles. However, increasing the concentration of BO decreased performance at higher power rates because the self-polymerizing oligomer thin film interrupted lithium-ion exchange. The structural changes in the cathode surface and electrolyte during charge/discharge cycles led to a high temperature cycle ability. Overall, this study investigated the influence of BO concentration on the electrochemical characteristics in lithium-ion cells and demonstrated the potential for using BO to provide a high temperature and long cycle life. The findings imply that the maleimide-based BO will undergo oxidation at a rate of 1.9 V relative to Li/Li⁺. The reference cells' discharge capacities were 143.2, 128.8, and 124.7 mAh g⁻¹ when they were discharged at a rate of 0.2 C.

According to Pan et al. [68], the occurrence of an explosion of a cell/battery is due to a chain of chemical reactions causing thermal runaway. The introduction of organic additives leads to the generation of a coating following a few rotations upon that cathode's interface, leading to a reduction in battery rate performance. Nonetheless, the suggested oligomer addition keeps a lithium battery's stability and cycle performance intact. Wang reported that the branched oligomer created a solid electrolyte interphase (SEI) during the charge/discharge mechanism of batteries. Furthermore, the results of the practical nail permeation test using prismatic cells show that the safety performance of a battery comprising branched oligomers incorporating (PMI)/BMI is preferable compared to the additive. Thus, the PMI/BMI-containing branched oligomer additive is demonstrated to improve the cycle ability, as well as the safety of LIBs.

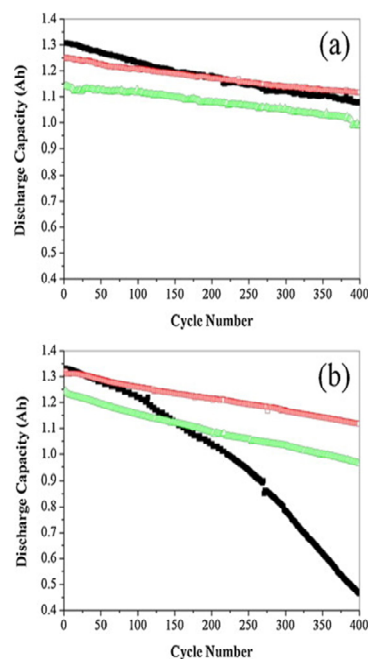


Figure 10. Cycle performance of Li-ion cells with BO as additives at 0.5 C: (a) at room temperature (25 °C); (b) at high temperature (55 °C); 1.0 M LiPF₆/EC:DEC, 1.0 M LiPF₆/EC:DEC + 1.0 wt% BO (BO₁), 1.0 M LiPF₆/EC:DEC + 2.5 wt% BO (BO₂);EC:DEC (6:4, v/v) [67].

According to Lin et al. [69], coating the surface of cathode active compounds with different inorganic interlayers has been highlighted, in certain circumstances, to reduce the exothermic interstitial interaction between the components of the electrolyte, as well as the cathode. To address the thermal breakdown limitation of LIBs, the ITRI, Taiwan, developed a polymeric cathode coating material of self-terminated oligomers with hyperbranched architecture. It has been demonstrated that this coating effectively suppresses thermal breakdown in the nail permeation methods of various graphite/oxide LIBs. Prior to the nail penetration test, the batteries were held under a constant current of 0.1 C between 4.2 V and 2.8 V and charged. LiO₂ cathode particles were coated with STOBA, which was demonstrated to successfully prevent thermal breakdown and mitigate the graphite potential difference. In situ synchrotron XRD analysis depicts that the polymer coating hardly impacted the layer-to-spinel phase orientation, suggesting that the suppressing methodology is working under the temperature of oxygen release from the oxide particles. The results from electrochemical as well as DSC analyses show that such a coating prefers to passively inhibit the interfacial tension of electrified cathode ions, which suppresses SEI development in a high-risk environment and significantly reduces the thermic potential arising from SEI breakdown, and when overheating, the electrified cathode layer decomposes the electrolyte.

Wen et al. [70] used nuclear magnetic resonance spectroscopy to conduct a study in the in situ setting and measure the equilibrium thermodynamics of the STOBA fabrication process. They researched the STOBA synthesizing procedure to identify important reactant locations, activation processes, and the effect of elements including the molecular level of the solution, the kind of reactant, the ratio, the volume, the activation time, the reaction duration, and the sequence of inclusion. Figure 11 [70] showed that the STOBA synthesis reaction follows primarily the Michael addition process, specifically a 2 + 2 stepwise polymerization. The α -methylene carbon as well as the two amino nitrogen atoms of benzene-1,3,5-tricarbaldehyde (BTA) are possible locations for nucleophiles that respond to the electrophilic C of N,N'-bismaleimide-4,4'-diphenylmethane. The STOBA preparation method has a relative pace comparable to that required for "Michael addition BTA > Knoevenagel condensation > self-reaction of MDA-BMI > self-polymerization of PMI". Experimental results revealed that the rate of reaction order is "BTA-BTA > BMI-BMI > PMI-PMI". This

study also concluded that now the Michael addition rule governs the chemical reactions of conflicting reaction processes of the rest, the BTA α -methylene proton retaliates with BMI/PMI C, Michael addition of the second BTA α -methylene proton reacts with the BMI/PMI $-\text{C}=\text{C}-$ double bond, and C1N0K to C1N0E tautomerization, BTA Knoevenagel condensation, MDA-BMI thermal polymerization, and PMI self-polymerization occur.

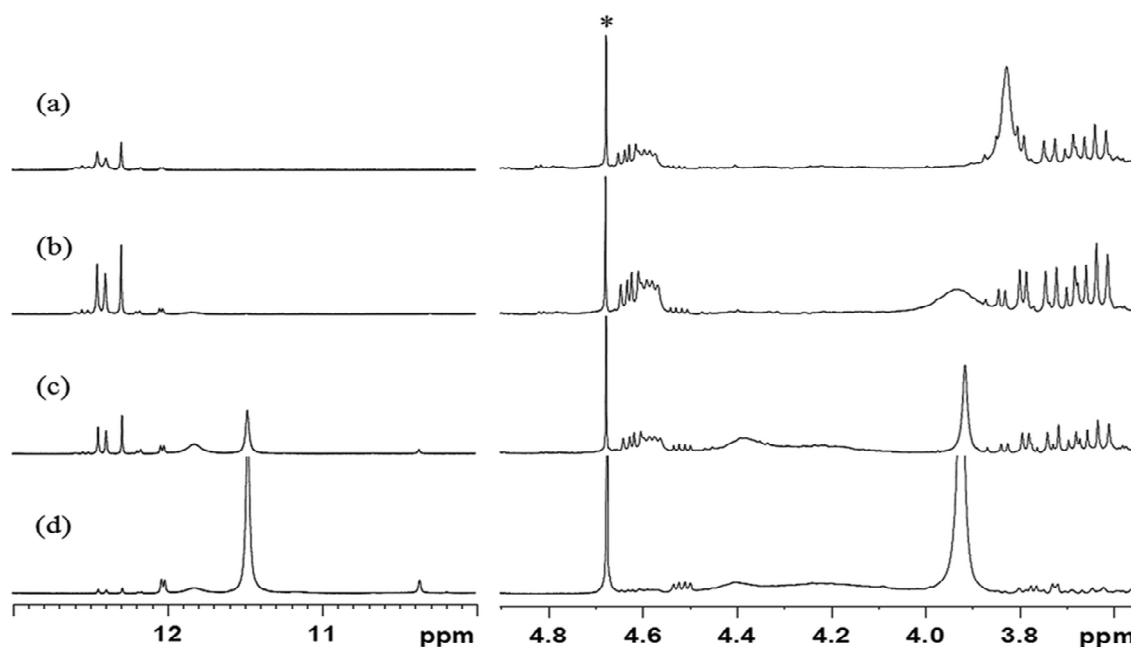


Figure 11. ^1H spectra of the reactions of PMI and BTA in ratios of (a) 4:1, (b) 2:1, (c) 1:1, and (d) 1:4 in solvent DMF at $90\text{ }^\circ\text{C}$. The peak with an asterisk on it is the residual proton signal of the inserted capillary filled with 99.9% D_2O [70].

Su et al. [71] developed a longitudinal reaction scenario whereby a silica particulate surface and a solitary siloxane bond were first created, in sync with condensation reactions between the silanol groups belonging to the silane molecules that are attached to the silica particle surface, in their study of the surface reaction of bistetrasulfane with silica. Silica enhanced the interaction seen between inorganic as well as organic fractions by connecting chemical organosilanes in addition to generating other desirable properties; for example, when employed as additives for different polymer composites, these properties include gas absorption, toughness, heat resistance, and scratch and wear resistance. Meanwhile, barbituric acid was utilized by Pan et al. to start the free radical polymerization of N,N' -bismaleimide-4,4'-diphenylmethane with two $-\text{C}=\text{C}-$. They found that the level of BTA initially controlled the polymerization, and the resulting oligomers with hyperbranches were soluble in organic solvents. The vinyltriethoxysilane molecule had already been effectively grafted onto silica nanoparticles according to the FTIR as well as TGA statistics. In their study, native along with silane-modified silica dispersions including continuous nonaqueous phase N -methyl-2-pyrrolidone and total solid contents ranging from 1 to 6 wt% exhibited a significantly different rheological mechanism.

In a study by Chern et al. [72], different solvents like N -methyl-2-pyrrolidinone, N,N' -dimethyl formamide, tetramethylsilane-containing dimethyl sulfoxide- d_6 , tetramethylsilane-containing chloroform- d_3 , and hydroquinone were used. A small amount of HQ was included in the mixture of the operation to polymerize BMI isothermally with 2,2'-Azobis(isobutyronitrile) (AIBN) to help establish the baseline during the primary stage of polymerization. The definition of the conversion was given as $X_{\text{DHT}} = \frac{\text{DH}}{\text{DH}_t}$, where DHT is indeed the region underneath the essential of the heat flow vs. t curve from t_0 to t , and the apparent total heat of the reaction resulting from the nonisothermal polymerization is represented by DH in the denominator. With this procedure, isothermal polymerization took place at 453 K

for one hour after the temperature was raised from room temperature to 453 K at a rate of 5 K min^{-1} . The reaction rate constant was in the range of 3.06×10^{-2} – $1.97 \times 10^{-11} / \text{min}$, and the activation energy was 76.3 kJ mol^{-1} in the 373–403 K temperature range. The study also included a discussion on the “mechanism of free radical polymerization of BMI triggered by BTA, involving initiation reactions, propagation reactions, and termination reactions, with a representative molecular structure corresponding to the resultant BMI polymer. The apparent overall heat of reaction per mole of BMI initially increased slowly up to a point where the mole fraction of BTA [BTA/ca] corresponds to nonisothermal polymerizations of BMI by BTA. Furthermore, at a specific weight percentage of HQ, the degree of DH reduction increased with the declining molar ratio of BTA/BMI. These results show that free radical polymer reactions contribute significantly to the polymerizations of BMI with BTA, alongside the Michael addition process.”

Yu et al. [73] found that barbituric acid or azobisisobutyronitrile can initiate the free radical polymerization of BMI. They observed that the overall heat of the reaction dropped rapidly and then leveled off as the concentration of HQ was elevated in nonisothermal polymerizations of BMI with BTA at various molar ratios of BTA/BMI. The study aimed to investigate the kinetics of Michael addition polymerization of BMI/BTA in NMP at various temperatures by incorporating enough HQ to inhibit the polymerization of free radicals. This made it possible to identify the actual critical kinetic parameters for Michael addition polymerization, such as the activation energy and reaction rate constants, by decoupling the intricate competitive Michael addition and free radical polymerization processes. The isothermal Michael addition polymerizations of *N,N'*-bismaleimide-4,4'-diphenylmethane, as well as barbituric acid, with BMI/BTA 2/1 in 1-methyl-2-pyrrolidone were explored independently by completely suppressing free radical polymer reactions through the addition of hydroquinone. The study developed in front of a crucial transformation. A mechanistic model was used to forecast the dynamics of polymerization; after that point, diffusion-controlled polymer reactions dominated throughout the latter stages of polymerization. Rate constants of Michael addition polymerization in the range of 2.44 – 7.18 L mol^{-1} for 21 min and an activation energy of 36.1 kJ mol^{-1} were obtained in the range of 383–423 K temperature based on the kinetic model. It was possible to reach a comparatively stationary limiting conversion beyond the critical conversion that was unaffected by the reaction temperature.

Pham et al. [74] showed that in the BMI-BTA polymerizations inside the temperature range of 100–130 °C, the Michael addition and free radical polymerization mechanisms competed with each other, with the input of the free radical polymerization mechanism increasing with reducing mole fraction of BTA in the medium of reaction. However, the key kinetic parameters of the Michael addition polymerization of BMI/BTA in the presence of HQ were significantly varied from those obtained in the mixed mode of competitive free radical and Michael addition polymerization mechanisms of BMI with BTA. In order to obtain a basic understanding of the thermal degradation process and mechanism, the aim of this study was to investigate the nonisothermal degradation kinetics of the cured samples of native BMI/BTA [2/1] and BMI/BTA in the presence of HQ in a solid state. They proposed a method to learn the kinetic parameters of the complex mechanism without resorting to the deconvolution technique. The cured polymer sample of S5 and its thermal breakdown process is primarily controlled by the simultaneous reaction order mechanism and third stage. Finally, for the cured polymer sample of S5, the model-fitting method yielded parameters of $E_a = 335.20 \text{ kJ mol}^{-1}$ and $c_A = 2.38 \times 10^{20} \text{ min}^{-1}$, corresponding to the thermal breakdown process involved in the third stage, with the greatest R_2 of 0.997 for $n = 1.45$ and $m = -1$.

Pham et al. [75] have reported that the mechanisms of free radical polymerization and Michael addition struggle amongst themselves in the polymerizations of BMI with BTA in the temperature range of 100–130 °C. The bequest of the free radical polymerization mechanism to the reaction of BMI with BTA elevates with reducing mole fraction of BTA in the reaction medium. In this work, they aimed to achieve a hybrid polymer

system of BMI/BTA and phenylsiloxane with adequate compatibility through the aid of 3-Aminopropyltriethoxysilane. Thermal stability was the focal point of this research for the PhSLX polymers. After satisfactory post-curing reactions, the PhSLX- and APTES (PASI)-altered BMI/BTA oligomers displayed diminished rates of thermal degradation in the range of 300–800 °C, increasing the level of residues at 800 °C compared to the native BMI/BTA oligomer. The activation energy values for the thermal degradation reactions of the cured PASI-modified BMI/BTA oligomers were found to be higher than those of the virgin BMI/BTA oligomer, as confirmed by additional thermal degradation kinetic tests. The Michael addition reaction between the amino group of APTES and the carbon–carbon double bonds of BMI allowed for the compatibility of the hybrid polymers of PhSLX and BMI/BTA oligomers. However, HYBRID30, comprising a greater level of the aminopropyl groups of APTES, displayed slightly lower thermic stability compared to HYBRID20, which could be ascribed to the thermal dependency of the cured PASI-modified BMI/BTA oligomers on the amounts of both PhSLX and APTES to some extent.

According to Pham and colleagues [76,77], the initiation mechanism for the BMI/BTA polymerization system involves the generation of a ketone radical pair via a single-electron transfer reaction. The authors aimed to examine the mechanism of nonisothermal degradation and the kinetics of the cured EA polymer, which was prepared via radical polymerization of EA triggered by either BTA or BPO. They used the deconvolution technique to estimate the distinct thermally oxidative degradation by utilizing a statistical function that addresses peaks on the differentiated thermogravimetric graph that are similar in size. They then conducted a kinetic analysis of the deconvoluted individual peaks to dictate the kinetic parameters, and the results were used to assess the relevant mechanisms. The values of activation energy (E_a) gained using the method of model fitting for the two primary thermal degradation steps of the cured polymer samples of BTA/EA, as well as BPO/EA, are comparable to those obtained from the model-free method, indicating that the degradation reaction mechanisms mentioned throughout this research are correct. The method of model fitting, aided by the deconvolution technique, was employed to determine the degradation kinetics for both cured polymer samples of BTA/EA and BPO/EA. As for the cured polymer sample of BPO/EA, reaction modulation was the mechanism guiding the initial stage of the deterioration process.

In their recent work, Pham et al. [78] proposed an initiation mechanism for the BMI/BTA polymerization system that involves the synthesis of a ketone radical pair through a single-electron migration reaction. They also investigated the distinction between the radical polymerization of EA started by conventional precursors like BPO and the polymerization of EA using BTA. The researchers focused on the molar ratio of BTA to EA as the major variable for the study. Their experiments showed that γ -butyrolactone (GBL), which lacks a nitrogen atom within its cyclic molecular structure, was unable to activate the radical polymerization of EA with BTA in the temperature range of 40–180 °C. In addition, the polymerization of EA with BTA in NMP or GBL did not exhibit a Michael addition reaction. The researchers found that the BTA concentration did not have a significant effect on the reaction mechanism for the polymerization of EA with BTA. Finally, based on the findings derived from the method of model fitting, the researchers proposed a first-stage reaction response process entailing nucleation and nucleus development.

Accelerating the cut-off voltage during charging has been suggested to enhance the density of energy in batteries. However, Yang et al. [79] reported that high voltage can cause unfavorable interphasial side reactions amidst the cathode, as well as the liquid electrolyte, leading to increased resistance, capacity loss, and cycle performance deterioration. To address this, oligomer additives were investigated as a means of reducing the endurance of electrochemical reactions by decreasing the polarization of the cell from the electrode surface. It was observed that the initial 10 cycles hold importance corresponding to the high-voltage cyclability of the batteries, as the high-voltage application of cells with BMI in the electrolyte was no different from that of cells with no additives when the batteries were directly cycled at a charging cut-off voltage of 4.5 V. The performance of high-voltage

cycling is primarily a result of three essential factors: cathode structure, cathode/electrolyte interphasial property, and electrolyte stability. In this experiment, the electrochemical stability of the electrolyte with BMI inclusion was up to 5.0 V, then a new interface film was formed on the cathode surface. This new interface film from BMI in the electrolyte served as a protective film that could effectively suppress unwanted interphasial side reactions within the cathode and liquid electrolyte. Consequently, BMI as an electrolytic addition considerably enhanced the LIBs' mechanical and physical properties.

Hydroquinone, a highly effective free radical inhibitor, was previously used by Yu et al. [80] as just a molecular tool to explore the dynamics and response mechanics of the polymerizations of BMI and BTA. A mechanistic model was subsequently improved to determine the Michael addition polymerization of BMI with BTA, taking into account the complicated competitive Michael addition reaction along with free radical polymerization mechanisms in the temperature range of 383–423 K. This was achieved by the addition of an adequate quantity of HQ to entirely suppress the competitive free radical polymerization. This study aims to investigate the impact of solvent proton affinity on the kinetics of Michael addition polymerization of BMI and BTA in solvents with different proton affinities at different temperatures. The isothermal Michael addition polymerizations of BMI and BTA with BMI/BTA (2/1) in different solvents in the temperature range of 383–423 K were studied, with the competitive free radical polymerization reactions completely suppressed by the addition of HQ. The activation energy of the Michael addition polymerization of BMI with BTA was correlated well with the solvent proton affinity and was found to be in the following order: "NMP < DMAC < DMF". This indicates that NMP, when at its highest proton affinity, was the most effective catalyst amidst the solvents investigated and greatly dropped the energy barrier for the Michael addition polymerization of BMI with BTA.

It has been reported by Pham et al. (2011) [81] that the Michael addition reaction mechanism allows BTA, which contains two > NH groups and one > CH₂ group, to polymerize with BMI. However, this process is not the only mechanism involved in the BMI/BTA polymerization, as there is also competition with free radical polymerization. Recently, it was found that adding 20 wt% aminopropyl phenylsiloxane oligomer (APSi) to BMI/BTA polymers enhances their thermal stability. The kinetics of polymerizations of BMI/BTA with the existence and deficiency of 20 wt% APSi were investigated, and the BMI content in BMI/BTA/APSi MPs was found to be 53 mol%, which is similar to that in BMI/BTA MPs.

In their previous work, Yu et al. [82] used hydroquinone as a molecular probe to investigate the reaction techniques and kinetics involved in the polymerizations of BMI with BTA by completely suppressing free radical polymerization. Working with the kinetic parameters of Michael addition polymerization, a mechanistic model was developed by combining experimental data from DSC and ¹H-NMR measurements to estimate the kinetic parameters of free radical polymerization initiated by BTA. The authors aimed to further investigate the contest between free radical polymerization and Michael addition polymerization in the polymerization of BMI with BTA by varying the molar ratio of BMI to BTA and the reaction temperature. They discovered that the polymerization of BMI with BTA involved a combination of processes, including Michael addition polymerization and free radical polymerization, and that the contribution of free radical polymerization increased with elevating temperature and molar ratio of BMI to BTA.

In 2016, Pham et al. [83] noted that BMI/BTA-based polymers with magnificent resistance to heat were being utilized as additives in LIBs, where preventing thermal runaway and explosion is a critical safety concern. Predicting the complexity of polymerization data arising from the simultaneous manifold steps requires the use of a deconvolution technique based on the supposition of the simple additivity of individual thermal effects, and the free radical and Michael addition reactions associated with the BMI/BTA system can be employed. The focal goal of this study is to investigate the nonisothermal polymerization mechanisms and kinetics included in the BMI/BTA system. Using the model-free method and the deconvolution technique, three different stages were identified in the BMI/BTA

polymerization system. The values of n for stages 1, 2, and 3 were determined to be 1.61 ± 0.02 , 2.24 ± 0.03 , and 2.77 ± 0.02 , respectively, using Erofeev models [84].

Chern et al. [85] reported that BMI/CA-based polymers can be effective additives for enhancing the performance of LIBs. This study aimed to understand the polymerization kinetics of BMI with CA in the presence of triethylamine and to provide useful data for the molecular design and scale-up of these BMI/CA-based polymers. The kinetics of polymerization of BMI with CA in NMP was studied for temperatures ranging from 50 to 80 °C, using both the model-free and model-fitting methods to ascertain the appropriate kinetic parameters. Comparable kinetic parameters were obtained by both techniques. The Michael addition mechanism included in the polymerization procedure of BMI/CA was successfully obtained by the model $g = \ln$ based on ^1H NMR measurements.

According to Chern et al. [86], while free radical polymerization was found to be the dominant mechanism in the polymerization of BMI with BTA in NMP, N,N' -dimethylacetamide, and N,N' -dimethylformamide, the Michael addition polymerization was governed by the $>\text{CH}_2$ group of BTA. The authors also investigated the processes and mechanisms of the reactions involved in polymerizing BMI in NMP using either 1,3-dimethylbarbituric acid or 5,5-dimethylbarbituric acid as displayed in the H-NMR spectra in Figure 12 [86]. Moreover, they studied the nonisothermal polymerization of BMI with BTA in DMSO and determined the triple kinetic parameters using the model-free and model-fitting methods. The current model obtained in the research study is consistent with that of Michael addition reactions.

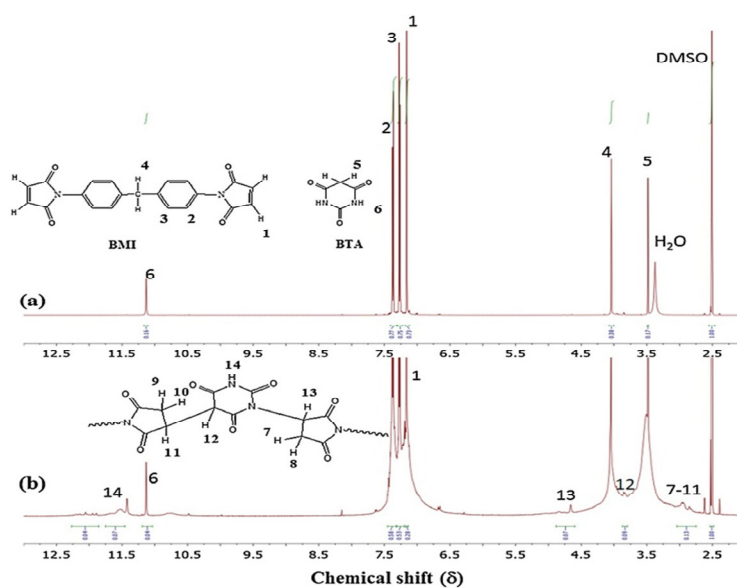


Figure 12. ^1H -NMR spectra for (a) the initial mixture of BMI/BTA [2/1 (mol/mol)] and (b) the resultant BMI/BTA polymer in $\text{DMSO-}d_6$ [86].

Wang and colleagues [87] reported the synthesis of two oligomers, named additive A and additive B, which were secured using the interaction reaction of BMI with 1,3-BTA and 5,5-BTA, respectively. The electrochemical and thermal properties of bare and modified NMC622 electrodes along with the two oligomers were explored. The phenomenon of interface kinetics was characterized based on the results of the surface plasma resonance. On the Au surface, additive B revealed a diminished intensity throughout the scanning due to the inhibition of the SP waves by the oligomer, whilst additive A showed an intermediate intensity due to the marginal excitement of the SPs. The study further investigated the operando gas evolution of the bare electrode, electrode A, and electrode B. The peak observed at approximately 536 eV was allocated to oxygen in Li_2CO_3 , which decreased in the surface-modified electrodes, with the intensity weakening at approximately 530.7 eV. The peak observed at 536 eV shifted drastically to a greater energy by 0.33 eV when the temperature increased from RT to 340 K, indicating that the generation of carbonate

species was remarkable at high temperatures. The electrode modification performed with additive B displayed optimal cycle performance, chiefly attributed to its stronger binding affinity at the electrode surface. Therefore, this study showed that additive B can efficiently inhibit degradation when LIBs are charged at large current voltages and temperatures, preventing electrolyte breakdown processes that produce residues and solidify the cathode morphology.

In their study, Wu et al. [88] found that LNCM cathode materials tend to exhibit structural and thermal instabilities when fully charged. This leads to decreased rate capability and poor capacity retention, mainly under high cut-off voltage and high-temperature conditions. To stop the surface of the cathode materials from one-to-one contact with the electrolyte, approaches, namely, coating of the surface and doping of the element, have been adopted. Coating materials, for example, metal oxide, phosphate, fluoride, or oligomer materials, can be applied to make a protective layer. The study investigated the effect of the concentration of BT oligomer species and the particle morphology of NCM523 active materials on the performance properties and safety of LIBs. The results revealed that the reaction mechanism involved in the polymerization of BT oligomers in the presence of NCM active materials differs from that in the absence of NCM cathode active materials. NCM523 active materials coated with varying amounts of BT oligomer as a bifunctional additive were successfully prepared for LIBs. The electrolyte decomposition temperature of the 1 wt% BT@NCM electrode was much higher than that of the bare LNCM electrode, and the heat generation of the coin cells with the 1 wt% BT@LNCM electrode in the completely charged state was minutely lower than that of the cells with the bare LNCM delithiated electrode, particularly when the temperature was increased from 25 to 300 °C. The study concluded that the BT oligomer is an effective bifunctional additive material for improving the performance and safety of LIBs.

Chong and colleagues [89] explained that nonuniform deposition of Li^+ on the Li electrode surface during charge can lead to the formation of undesirable Li dendrites, which may penetrate the separator and cause a short circuit. To prevent contact between the two electrodes and to allow movement of Li^+ during the process of charge/discharge, microporous polymeric separator membranes are used in LIBs. The separator also affects the electrochemical performance properties and safety. After a long cycling process, the bare Li metal anode may develop a rough surface morphology and fissures and generate a huge number of byproducts due to side reactions with the electrolyte. The stated negative factors contribute to the buildup of Li metal in the structure, which is porous and loose, that in turn increases the interfacial resistance, as well as the capacity fading rate. To design polymer materials that can suppress Li dendrite development on the Li metal anode surface during cycling of the Li metal battery, factors including the uniform distribution of Li^+ flux, blocking of Li dendrites' mechanical formation, and polymer structure tailoring, along with modulating the physical structure of polymer membranes, should be taken into account. However, the mechanisms related to the safety of LIBs with a reactive polymer coated on the cathode active material pellet surface are unclear.

Additionally, because of the collapse of the SEI upon that anode surface, thermal runaway results in a tremendous declination of the electrolyte. To avoid thermal runaway, which is primarily caused by the ferociously exothermic interaction of the combustible electrolyte with the cathode only, but also results in oxygen evolution out of the cathode, it is imperative to have a solid grasp of how to manage the amount of heat produced. Earlier research has concentrated on decreasing the volatile character of the electrolytes by including additives, including cosolvents, in the electrolytes in the hope of decreasing similar effects. Moreover, it has been shown that flame-retardant electrolytes containing additional fire retardants diminish the combustibility of the electrolyte. These fire retardants' combination with active elements in the electrodes, nevertheless, causes them to have additional detrimental impacts on battery efficiency. New findings mention many monomer additions that polymerize to create electrical conducting polymers under cell voltages higher than the optimum operational voltage level. An ITRI-developed nanos-

structured polymeric electrode coating compound called STOBA apparently successfully reduces thermal runaway under abusive circumstances in an LIB. According to a study, STOBA change from permeable substances to a coating and halts the process whenever the battery reaches 130 °C. Without any discernible impact upon electrochemical properties, 2% of STOBA may effectively cover the whole surface layer, thus preventing thermal runaway. They possess the capacity to create a stable combination with the electroactive component only due to their hyperbranched features. They also improve adherence to the electrode, as well as the contemporary collector, and are compatible with the electrolytes. The layer of STOBA has no impact on the transport of lithium ions during cycling in an ambient environment. The STOBA strands that have been formed upon the cell's interface crosslink as the temperature rises, becoming nonporous but hard. This prevents the electrolytes from coming into contact with oxygen directly, preventing the electrolyte from decomposing. Furthermore, the polymerization and layer transition from a permeable to a nonporous state following heating prevent both the movement of lithium ions and electrons. The layer-to-spinel transition region is unaffected by the STOBA coating upon $\text{Li}(\text{Ni}_{0.4}\text{Co}_{0.2}\text{Mn}_{0.4})\text{O}_2$ because electrolyte breakdown is prevented before the oxide layer even releases oxygen. Furthermore, electrolyte additives offer a useful way to increase the compatibility among electrolytes with cathode phases. Subsequently, an electrolytic additive for LIBs called STOBA—a branched bismaleimide oligomer—was used. According to a paper, the oligomer supplement can lessen the intractability of electrochemical processes by reducing the orientation of the device away from the working electrode. There are not many publications on the method; however, there are a few descriptions that explain how STOBA ends thermal runaway. Additionally, investigation on the reconfiguration of STOBA with different functional groups or novel emulsifiers with comparable physical and chemical characteristics, including such additives that do not initiate reaction during storage or operational phases but initiate crosslinking at a specific temperature, could prove to be a productive prospective research area.

5. Conclusions and Future Work

In conclusion, STOBA materials have the potential to be next-generation additives in anode and cathode materials for LIBs due to their unique properties such as high specific capacity, low impedance, excellent cycling stability, and mechanical stability. Their unique hyperbranched structure contributes to these properties. Current research efforts are aimed at improving their synthesis methods, increasing their specific capacity, improving their cycling stability, and reducing the cost of the materials. These efforts will help to optimize STOBA materials for use in LIBs and make them more practical for various applications. While there has been significant progress in understanding the properties and potential applications of STOBA materials, there are still several areas for further research. In this article, we discussed some of the key areas for further research, including the optimization of synthesis processes, investigation of long-term stability and safety, and the use of advanced techniques such as in situ spectroscopy and electrochemistry. One important area for further research is the optimization of synthesis and characterization of STOBA materials. The synthesis of STOBA materials is currently challenging, and researchers are working on developing methods to improve the control of the degree of branching during synthesis. This would allow for more precise control of the properties of the resulting material. In addition, researchers are working on developing new characterization techniques to better understand the properties of STOBA materials. Another important area for further research is the investigation of the long-term stability and safety of STOBA materials. While STOBA materials have excellent cycling stability, it is important to investigate their long-term stability over many charge and discharge cycles. Additionally, researchers need to investigate the safety of STOBA materials, especially in the event of thermal runaway or other accidents. A third area for further research is the use of advanced techniques such as in situ spectroscopy and electrochemistry to study the properties of STOBA materials. These techniques allow researchers to study the materials in real time and under realistic

conditions, which can provide valuable information about their properties and behavior. In conclusion, while there has been significant progress in understanding the properties and potential applications of STOBA materials, there are still several areas for further research. These include the optimization of synthesis and characterization, investigation of long-term stability and safety, and the use of advanced techniques such as in situ spectroscopy and electrochemistry. These efforts will help us to fully understand the properties of STOBA materials and to develop methods for their practical applications in LIBs.

Author Contributions: Conceptualization, D.M. and C.-T.H.; methodology and writing—original draft preparation, D.M.; validation, W.-R.L., I.-M.H. and J.-P.P.; writing—review and editing, C.-T.H., I.-M.H. and W.-R.L.; supervision, C.-T.H. and I.-M.H.; funding acquisition, C.-T.H., I.-M.H. and W.-R.L. All authors have read and agreed to the published version of the manuscript.

Funding: The authors gratefully acknowledge the support of the Ministry of Science and Technology in Taiwan, provided through grant number NSTC 112-2221-E-155-005-MY3.

Data Availability Statement: No new data were created or analyzed in this study. Data sharing is not applicable to this article.

Acknowledgments: The authors gratefully acknowledge the support of the National of Science and Technology Council (NTSC) in Taiwan, provided through grant numbers NSTC 112-2221-E-155-005-MY3, 112-2218-E-007-023, 111-2622-E-033-007, 111-2923-E-006-009, 112-2218-E-007-023, and 111-2221-E-033 -004 -MY3.

Conflicts of Interest: The authors declare no conflicts of interest.

References

1. Parlikar, A.; Schott, M.; Godse, K.; Kucevic, D.; Jossen, A.; Hesse, H. High-power electric vehicle charging: Low-carbon grid integration pathways with stationary lithium-ion battery systems and renewable generation. *Appl. Energy* **2023**, *333*, 120541–120557. [[CrossRef](#)]
2. Pražanová, A.; Knap, V.; Stroe, D.I. Literature Review, Recycling of Lithium-Ion Batteries from Electric Vehicles, Part II: Environmental and Economic Perspective. *Energies* **2022**, *15*, 7356. [[CrossRef](#)]
3. San Román, T.G.; Momber, I.; Abbad, M.R.; Sánchez Miralles, A. Regulatory framework and business models for charging plug-in electric vehicles: Infrastructure, agents, and commercial relationships. *Energy Pol.* **2011**, *39*, 6360–6375. [[CrossRef](#)]
4. Rangarajan, S.S.; Sundararaj, S.P.; Sudhakar, A.V.V.; Siva, C.K.; Subramaniam, U.; Collins, E.R.; Senjyu, T. Lithium-Ion Batteries—The Crux of Electric Vehicles with Opportunities and Challenges. *Clean Technol.* **2022**, *4*, 908–930. [[CrossRef](#)]
5. Fang, R.; Chen, K.; Yin, L.; Sun, Z.; Li, F.; Cheng, H.M. The Regulating Role of Carbon Nanotubes and Graphene in Lithium-Ion and Lithium–Sulfur Batteries. *Adv. Mater.* **2019**, *31*, 1800863–1800884. [[CrossRef](#)]
6. Wu, F.; Maier, J.; Yu, Y. Guidelines and trends for next-generation rechargeable lithium and lithium-ion batteries. *Chem. Soc. Rev.* **2020**, *49*, 1569–1614. [[CrossRef](#)]
7. Wagner, R.; Preschitschek, N.; Passerini, S.; Leker, J.; Winter, M. Current research trends and prospects among the various materials and designs used in lithium-based batteries. *J. Appl. Electrochem.* **2013**, *43*, 481–496. [[CrossRef](#)]
8. Cavers, H.; Molaiyan, P.; Abdollahifar, M.; Lassi, U.; Kwade, A. Perspectives on Improving the Safety and Sustainability of High Voltage Lithium-Ion Batteries Through the Electrolyte and Separator Region. *Adv. Energy Mater.* **2022**, *12*, 2200147–2200179. [[CrossRef](#)]
9. Chombo, P.V.; Laonual, Y. A review of safety strategies of a Li-ion battery. *J. Power Sources* **2020**, *478*, 228649–228666. [[CrossRef](#)]
10. Chen, Y.; Kang, Y.; Zhao, Y.; Wang, L.; Liu, J.; Li, Y.; Liang, Z.; He, X.; Li, X.; Tavajohi, N.; et al. A review of lithium-ion battery safety concerns: The issues, strategies, and testing standards. *J. Energy Chem.* **2021**, *59*, 83–99. [[CrossRef](#)]
11. Qiu, Y.; Jiang, F. A review on passive and active strategies of enhancing the safety of lithium-ion batteries. *Int. J. Heat. Mass Trans.* **2022**, *184*, 122288–122301. [[CrossRef](#)]
12. Liu, Y.; Duan, Q.; Xu, J.; Li, H.; Sun, J.; Wang, Q. Experimental study on a novel safety strategy of lithium-ion battery integrating fire suppression and rapid cooling. *J. Energy Storage* **2020**, *28*, 101185–101193. [[CrossRef](#)]
13. Md Said, M.S.; Mohd Tohir, M.Z. Visual and thermal imaging of lithium-ion battery thermal runaway induced by mechanical impact. *J. Loss Prev. Proc. Indust.* **2022**, *79*, 104854–104861. [[CrossRef](#)]
14. Goodman, J.K.S.; Miller, J.T.; Kreuzer, S.; Forman, J.; Wi, S.; Choi, J.M.; Oh, B.; White, K. Lithium-ion cell response to mechanical abuse: Three-point bend. *J. Energy Storage* **2020**, *28*, 101244–101254. [[CrossRef](#)]
15. Feng, X.; Ouyang, M.; Liu, X.; Lu, L.; Xia, Y.; He, X. Thermal runaway mechanism of lithium ion battery for electric vehicles: A review. *Energy Storage Mater.* **2018**, *10*, 246–267. [[CrossRef](#)]
16. Feng, X.; Ren, D.; He, X.; Ouyang, M. Mitigating Thermal Runaway of Lithium-Ion Batteries. *Joule* **2020**, *4*, 743–770. [[CrossRef](#)]

17. Xu, B.; Lee, J.; Kwon, D.; Kong, L.; Pecht, M. Mitigation strategies for Li-ion battery thermal runaway: A review. *Renew. Sustain. Energy Rev.* **2021**, *150*, 111437–111459. [[CrossRef](#)]
18. Larsson, F.; Andersson, P.; Mellander, B.E. Lithium-Ion Battery Aspects on Fires in Electrified Vehicles on the Basis of Experimental Abuse Tests. *Batteries* **2016**, *2*, 9. [[CrossRef](#)]
19. Rajmakers, L.H.J.; Danilov, D.L.; Eichel, R.A.; Notten, P.H.L. A review on various temperature-indication methods for Li-ion batteries. *Appl. Energy* **2019**, *240*, 918–945. [[CrossRef](#)]
20. Gabryelczyk, A.; Ivanov, S.; Bund, A.; Lota, G. Corrosion of aluminium current collector in lithium-ion batteries: A review. *J. Energy Storage* **2021**, *43*, 103226–103247. [[CrossRef](#)]
21. Yuan, M.; Liu, K. Rational design on separators and liquid electrolytes for safer lithium-ion batteries. *J. Energy Chem.* **2020**, *43*, 58–70. [[CrossRef](#)]
22. Mohanty, D.; Chen, S.Y.; Hung, I.M. Effect of Lithium Salt Concentration on Materials Characteristics and Electrochemical Performance of Hybrid Inorganic/Polymer Solid Electrolyte for Solid-State Lithium-Ion Batteries. *Batteries* **2022**, *8*, 173. [[CrossRef](#)]
23. Feng, T.; Guo, W.; Li, Q.; Meng, Z.; Liang, W. Life cycle assessment of lithium nickel cobalt manganese oxide batteries and lithium iron phosphate batteries for electric vehicles in China. *J. Energy Storage* **2022**, *52*, 104767–104778. [[CrossRef](#)]
24. Nitta, N.; Wu, F.; Lee, J.T.; Yushin, G. Li-ion battery materials: Present and future. *Mater. Today* **2015**, *18*, 252–264. [[CrossRef](#)]
25. Hagen, M.; Hanselmann, D.; Ahlbrecht, K.; Maça, R.; Gerber, D.; Tübke, J. Lithium–Sulfur Cells: The Gap between the State-of-the-Art and the Requirements for High Energy Battery Cells. *Adv. Energy Mater.* **2015**, *5*, 1401986–1401996. [[CrossRef](#)]
26. Koerver, R.; Aygün, I.; Leichtwei, T.; Dietrich, C.; Zhang, W.; Binder, J.O.; Hartmann, P.; Zeier, W.G.; Janek, J. Capacity Fade in Solid-State Batteries: Interphase Formation and Chemomechanical Processes in Nickel-Rich Layered Oxide Cathodes and Lithium Thiophosphate Solid Electrolytes. *Chem. Mater.* **2017**, *29*, 5574–5582. [[CrossRef](#)]
27. Costa, C.M.; Barbosa, J.C.; Gonçalves, R.; Castro, H.; Campo, F.J.G.; Lanceros-Méndez, S. Recycling and environmental issues of lithium-ion batteries: Advances, challenges and opportunities. *Energy Storage Mater.* **2021**, *37*, 433–465. [[CrossRef](#)]
28. Mukherjee, A.B.; Zevenhoven, R.; Brodersen, J.; Hylander, L.D.; Bhattacharya, P. Mercury in waste in the European Union: Sources, disposal methods and risks. *Res. Conserv. Recycl.* **2004**, *42*, 155–182. [[CrossRef](#)]
29. Huang, L.; Liu, L.; Lu, L.; Feng, X.; Han, X.; Li, W.; Zhang, M.; Li, D.; Liu, X.; Sauer, D.U.; et al. A review of the internal short circuit mechanism in lithium-ion batteries: Inducement, detection and prevention. *Int. J. Energy Res.* **2021**, *45*, 15797–15831. [[CrossRef](#)]
30. Pham, Q.T.; Hsu, J.M.; Pan, J.P.; Wang, T.H.; Chern, C.S. Synthesis and characterization of phenylsiloxane-modified bis-maleimide/barbituric acid-based polymers with 3-aminopropyltriethoxysilane as the coupling agent. *Polymer Int.* **2013**, *62*, 1045–1052. [[CrossRef](#)]
31. Lai, X.; Jin, C.; Yi, W.; Han, X.; Feng, X.; Zheng, Y.; Ouyang, M. Mechanism, modeling, detection, and prevention of the internal short circuit in lithium-ion batteries: Recent advances and perspectives. *Energy Storage Mater.* **2021**, *35*, 470–499. [[CrossRef](#)]
32. Wen, L.; Liang, J.; Chen, J.; Chu, Z.Y.; Cheng, H.M.; Li, F. Smart Materials and Design toward Safe and Durable Lithium Ion Batteries. *Small Methods* **2019**, *3*, 1900323–1900354. [[CrossRef](#)]
33. Finegan, D.P.; Darcy, E.; Keyser, M.; Tjaden, B.; Heenan, T.M.M.; Jervis, R.; Baily, J.J.; Malik, R.; Vo, N.T.; Magdysyuk, O.V.; et al. Characterising thermal runaway within lithium-ion cells by inducing and monitoring internal short circuits. *Energy Environ. Sci.* **2017**, *10*, 1377–1388. [[CrossRef](#)]
34. Zhu, L.; Ding, G.; Han, Q.; Yang, X.; Xie, L.; Cao, X. Review—Recent Developments in Safety-Enhancing Separators for Lithium-Ion Batteries. *J. Electrochem. Soc.* **2021**, *168*, 100524–100542. [[CrossRef](#)]
35. Wang, F.; Hu, E.; Sun, W.; Gao, T.; Ji, X.; Fan, X.; Han, F.; Yang, X.Q.; Xu, K.; Wang, C. A rechargeable aqueous Zn²⁺-battery with high power density and a long cycle-life. *Energy Environ. Sci.* **2018**, *11*, 3168–3175. [[CrossRef](#)]
36. Wu, H.B.; Chen, J.S.; Hng, H.H.; Lou, X.W. Nanostructured metal oxide-based materials as advanced anodes for lithium-ion batteries. *Nanoscale* **2012**, *4*, 2526–2542. [[CrossRef](#)] [[PubMed](#)]
37. Yu, L.; Wang, D.; Zhao, Z.; Han, J.; Zhang, K.; Cui, X.; Xu, Z. Pore-forming Technology Development of Polymer Separators for Power Lithium-ion Battery. In *Proceedings of the SAE-China Congress 2014: Selected Papers*; Lecture Notes in Electrical Engineering; Springer: Berlin/Heidelberg, Germany, 2015; pp. 71–80.
38. Cui, X.; Mi, X.; Cao, T.; Jiang, T.; Chen, H.; Zhao, Z.; Zhang, K. Studies on the Working Mode of Hyperbranched New Materials STObA in Lithium-ion Battery Cathode Materials. In *Proceedings of the SAE-China Congress 2014: Selected Papers*; Lecture Notes in Electrical Engineering; Springer: Berlin/Heidelberg, Germany, 2015; pp. 81–88.
39. Wang, Y.W.; Shu, C.M. Hazard Characterizations of Li-Ion Batteries: Thermal Runaway Evaluation by Calorimetry Methodology. In *Rechargeable Batteries: Materials, Technologies and New Trends*, 1st ed.; Zhang, Z., Zhang, S., Eds.; Springer International Publishing: Cham, Switzerland, 2015; pp. 419–454.
40. Shi, X.; Simanova, E.; Schönherr, J.; Schreiber, L. Effects of Accelerators on Mobility of 14C-2,4-Dichlorophenoxy Butyric Acid in Plant Cuticles Depends on Type and Concentration of Accelerator. *J. Agric. Food Chem.* **2005**, *53*, 2207–2212. [[CrossRef](#)] [[PubMed](#)]
41. Ma, P.; Dai, C.; Wang, H.; Li, Z.; Liu, H.; Li, W.; Yang, C. A review on high temperature resistant polyimide films: Heterocyclic structures and nanocomposites. *Comp. Commun.* **2019**, *16*, 84–93. [[CrossRef](#)]
42. Guarneri, A.; Cutifani, V.; Cespugli, M.; Pellis, A.; Vasallo, R.; Asaro, F.; Ebert, C.; Gardossi, L. Functionalization of Enzymatically Synthesized Rigid Poly(itaconate)s via Post-Polymerization Aza-Michael Addition of Primary Amines. *Adv. Synth. Catal.* **2019**, *361*, 2559–2573. [[CrossRef](#)]

43. Writer, B. Ionic Conductivity, Polymer Electrolyte, Membranes, Electrochemical Stability, Separators. In *Lithium-Ion Batteries: A Machine-Generated Summary of Current Research*, 1st ed.; Writer, B., Ed.; Springer International Publishing: Cham, Switzerland, 2019; pp. 163–193.
44. Pintauer, T.; Braunecker, W.; Collange, E.; Poli, R.; Matyjaszewski, K. Determination of Rate Constants for the Activation Step in Atom Transfer Radical Polymerization Using the Stopped-Flow Technique. *Macromolecules* **2004**, *37*, 2679–2682. [[CrossRef](#)]
45. Sun, G.; Cheng, C.; Wooley, K.L. Reversible Addition Fragmentation Chain Transfer Polymerization of 4-Vinylbenzaldehyde. *Macromolecules* **2007**, *40*, 793–795. [[CrossRef](#)] [[PubMed](#)]
46. Martinez, H.; Ren, N.; Matta, M.E.; Hillmyer, M.A. Ring-opening metathesis polymerization of 8-membered cyclic olefins. *Polym. Chem.* **2014**, *5*, 3507–3532. [[CrossRef](#)]
47. Chen, J.; Spear, S.K.; Huddleston, J.G.; Rogers, R.D. Polyethylene glycol and solutions of polyethylene glycol as green reaction media. *Green Chem.* **2005**, *7*, 64–82.
48. Aoshima, H.; Uchiyama, M.; Satoh, K.; Kamigaito, M. Interconvertible Living Radical and Cationic Polymerization through Reversible Activation of Dormant Species with Dual Activity. *Angew. Chem. Int. Ed.* **2014**, *53*, 10932–10936. [[CrossRef](#)] [[PubMed](#)]
49. Zhao, K.; Song, H.; Duan, X.; Wang, Z.; Liu, J.; Ba, X. Novel Chemical Cross-Linked Ionogel Based on Acrylate Terminated Hyperbranched Polymer with Superior Ionic Conductivity for High Performance Lithium-Ion Batteries. *Polymers* **2019**, *11*, 444. [[CrossRef](#)] [[PubMed](#)]
50. Li, Y.; Qiu, W.; Qin, F.; Fang, H.; Hadjiev, V.G.; Litvinov, D.; Bao, J. Identification of Cobalt Oxides with Raman Scattering and Fourier Transform Infrared Spectroscopy. *J. Phys. Chem. C* **2016**, *120*, 4511–4516. [[CrossRef](#)]
51. Hari, B.S.; Kumar, K.V.M.; Krishnamurthy, K.; Kumar, P.S.; Gobinath, V.K.; Sachinbala, R.; Rajasekar, R. Influence of graphene oxide on the morphological and mechanical behaviour of compatibilized low density polyethylene nanocomposites. *Mater. Today Proceed.* **2021**, *39*, 1487–1493.
52. Martinez-Cisneros, C.S.; Fernandez, A.; Antonelli, C.; Levenfeld, B.; Varez, A.; Vezzu, K.; Di Noto, V.; Sanchez, J.Y. Opening the door to liquid-free polymer electrolytes for calcium batteries. *Electrochim. Acta* **2020**, *353*, 136525–136535. [[CrossRef](#)]
53. Tian, X.; Yi, Y.; Fang, B.; Yang, P.; Wang, T.; Liu, P.; Qu, L.; Li, M.; Zhang, S. Design Strategies of Safe Electrolytes for Preventing Thermal Runaway in Lithium Ion Batteries. *Chem. Mater.* **2020**, *32*, 9821–9848. [[CrossRef](#)]
54. Xie, J.; Lu, Y.C. A retrospective on lithium-ion batteries. *Nat. Commun.* **2020**, *11*, 2499–2502. [[CrossRef](#)]
55. Thalji, M.R.; Ibrahim, A.A.; Ali, G.A.M. Cutting-edge development in dendritic polymeric materials for biomedical and energy applications. *Eur. Polym. J.* **2021**, *160*, 110770–110794. [[CrossRef](#)]
56. Yue, L.; Ma, J.; Zhang, J.; Zhao, J.; Dong, S.; Liu, Z.; Cui, G.; Chen, L. All solid-state polymer electrolytes for high-performance lithium ion batteries. *Energy Storage Mater.* **2016**, *5*, 139–164. [[CrossRef](#)]
57. Wang, Y.; Xu, Y.; Ma, S.; Duan, R.; Zhao, Y.; Zhang, Y.; Liu, Z.; Li, C. Low temperature performance enhancement of high-safety Lithium–Sulfur battery enabled by synergetic adsorption and catalysis. *Electrochim. Acta* **2020**, *353*, 136470–136480. [[CrossRef](#)]
58. Haregewoin, A.M.; Wotango, A.S.; Hwang, B.J. Electrolyte additives for lithium ion battery electrodes: Progress and perspectives. *Energy Environ. Sci.* **2016**, *9*, 1955–1988. [[CrossRef](#)]
59. Spotte-Smith, E.W.S.; Kam, R.L.; Barter, D.; Xie, X.; Hou, T.; Dwaraknath, S.; Blau, S.M.; Persson, K.A. Toward a Mechanistic Model of Solid–Electrolyte Interphase Formation and Evolution in Lithium-Ion Batteries. *ACS Energy Lett.* **2022**, *7*, 1446–1453. [[CrossRef](#)]
60. Kowalczyk, S.; Dębowski, M.; Iuliano, A.; Brzeski, S.; Plichta, A. Synthesis of (Hyper)Branched Monohydroxyl Alkoxysilane Oligomers toward Silanized Urethane Prepolymers. *Molecules* **2012**, *27*, 2790–2806. [[CrossRef](#)] [[PubMed](#)]
61. Feng, X.; Zheng, S.; Ren, D.; He, X.; Wang, L.; Cui, H.; Liu, X.; Jin, C.; Zhang, F.; Xu, C.; et al. Investigating the thermal runaway mechanisms of lithium-ion batteries based on thermal analysis database. *Appl. Energy* **2019**, *246*, 53–64. [[CrossRef](#)]
62. Liu, K.; Liu, Y.; Lin, D.; Pei, A.; Cui, Y. Materials for lithium-ion battery safety. *Sci. Adv.* **2018**, *4*, 9820–9830. [[CrossRef](#)]
63. Liu, H.M.; Saikia, D.; Wu, H.C.; Su, C.Y.; Wang, T.H.; Li, Y.H.; Pan, J.P.; Kao, H.M. Towards an understanding of the role of hyper-branched oligomers coated on cathodes, in the safety mechanism of lithium-ion batteries. *RSC Adv.* **2014**, *4*, 56147–56155. [[CrossRef](#)]
64. Duh, Y.S.; Sun, Y.; Lin, X.; Zheng, J.; Wang, W.; Wang, Y.; Lin, X.; Jiang, X.; Zheng, Z.; Zheng, S.; et al. Characterization on thermal runaway of commercial 18650 lithium-ion batteries used in electric vehicles: A review. *J. Energy Storage* **2021**, *41*, 102888–102902. [[CrossRef](#)]
65. Pham, Q.T.; Hsu, J.M.; Shao, W.J.; Wang, F.M.; Chern, C.S. Mechanisms and kinetics of isothermal polymerization of N,N'-bismaleimide-4,4'-diphenylmethane with 5,5-dimethylbarbituric acid in the presence of triphenylphosphine. *Thermochim. Acta* **2017**, *655*, 234–241. [[CrossRef](#)]
66. Pham, Q.T.; Hsu, J.M.; Shao, W.J.; Zhan, Y.X.; Wang, F.M.; Chern, C.S. Mechanisms and kinetics of non-isothermal polymerization of N,N'-bismaleimide-4,4'-diphenylmethane with 1,3-dimethylbarbituric acid. *Thermochim. Acta* **2017**, *658*, 31–37. [[CrossRef](#)]
67. Li, Y.H.; Lee, M.L.; Wang, F.M.; Yang, C.R.; Chu, P.P.J.; Pan, J.P. Electrochemical characterization of a branched oligomer as a high-temperature and long-cycle-life additive for lithium-ion batteries. *Electrochim. Acta* **2012**, *85*, 72–77. [[CrossRef](#)]
68. Li, Y.H.; Lee, M.L.; Wang, F.M.; Yang, C.R.; Chu, P.P.J.; Yau, S.L.; Pan, J.P. Electrochemical performance and safety features of high-safety lithium ion battery using novel branched additive for internal short protection. *Appl. Surf. Sci.* **2012**, *261*, 306–311. [[CrossRef](#)]

69. Lin, C.C.; Wu, H.C.; Pan, J.P.; Su, C.Y.; Wang, T.H.; Sheu, H.S.; Wu, N.L. Investigation on suppressed thermal runaway of Li-ion battery by hyper-branched polymer coated on cathode. *Electrochim. Acta* **2013**, *101*, 11–17. [[CrossRef](#)]
70. Wen, Y.C.; Sue, Y.C.; Yang, S.Y.; Pan, J.P.; Wang, T.H.; Jia, H.W. NMR spectroscopy study on N,N'-bismaleimide-4,4'-diphenylmethane and barbituric acid synthesis reaction mechanism in N,N'-dimethylformamide solvent. *RSC Adv.* **2017**, *7*, 651–661. [[CrossRef](#)]
71. Su, H.L.; Hsu, J.M.; Pan, J.P.; Chern, C.S. Silica nanoparticles modified with vinyltriethoxysilane and their copolymerization with N,N'-bismaleimide-4,4'-diphenylmethane. *J. Appl. Polymer Sci.* **2007**, *103*, 3600–3608. [[CrossRef](#)]
72. Wang, F.M.; Cheng, H.M.; Wu, H.C.; Chu, H.Y.; Cheng, C.S.; Yang, C.R. Novel SEI formation of maleimide-based additives and its improvement of capability and cyclicability in lithium ion batteries. *Electrochim. Acta* **2009**, *54*, 3344–3351. [[CrossRef](#)]
73. Su, H.L.; Hsu, J.M.; Pan, J.P.; Wang, T.H.; Chern, C.S. Effects of solvent basicity on free radical polymerizations of N,N'-bismaleimide-4,4'-diphenylmethane initiated by barbituric acid. *J. Appl. Polymer Sci.* **2010**, *117*, 596–603. [[CrossRef](#)]
74. Su, H.L.; Hsu, J.M.; Pan, J.P.; Wang, T.H.; Yu, F.E.; Chern, C.S. Kinetic and structural studies of the polymerization of N,N'-bismaleimide-4,4'-diphenylmethane with barbituric acid. *Polymer Eng. Sci.* **2011**, *51*, 1188–1197. [[CrossRef](#)]
75. Yu, F.E.; Hsu, J.M.; Pan, J.P.; Wang, T.H.; Chern, C.S. Kinetics of Michael addition polymerizations of n,n'-bismaleimide-4,4'-diphenylmethane with barbituric acid. *Polymer Eng. Sci.* **2013**, *53*, 204–211. [[CrossRef](#)]
76. Pham, Q.T.; Hsu, J.M.; Pan, J.P.; Wang, T.H.; Chern, C.S. Non-isothermal degradation kinetics of N,N'-bismaleimide-4,4'-diphenylmethane/barbituric acid based polymers in the presence of hydroquinone. *J. Appl. Polymer Sci.* **2013**, *130*, 1923–1930. [[CrossRef](#)]
77. Pham, Q.T.; Hsu, J.M.; Pan, J.P.; Wang, T.H.; Chern, C.S. Non-isothermal degradation of bisphenol A diglycidyl ether diacrylate-based polymers. *Thermochim. Acta* **2013**, *573*, 10–17. [[CrossRef](#)]
78. Pham, Q.T.; Hsu, J.M.; Pan, J.P.; Wang, T.H.; Chern, C.S. Kinetics of free radical polymerization of bisphenol A diglycidyl ether diacrylate initiated by barbituric acid. *Thermochim. Acta* **2013**, *573*, 121–129. [[CrossRef](#)]
79. Yang, J.; Zhao, P.; Shang, Y.; Wang, L.; He, X.; Fang, M.; Wang, J. Improvement in High-voltage Performance of Lithium-ion Batteries Using Bismaleimide as an Electrolyte Additive. *Electrochim. Acta* **2014**, *121*, 264–269. [[CrossRef](#)]
80. Yu, F.E.; Hsu, J.M.; Pan, J.P.; Wang, T.H.; Chiang, Y.C.; Lin, W.; Jiang, J.C.; Chern, C.S. Effect of solvent proton affinity on the kinetics of michael addition polymerization of n,n'-bismaleimide-4,4'-diphenylmethane with barbituric acid. *Polymer Eng. Sci.* **2014**, *54*, 559–568. [[CrossRef](#)]
81. Pham, Q.T.; Yu, F.E.; Hsu, J.M.; Chiang, C.H.; Chern, C.S. Kinetics of polymerization of N,N'-bismaleimide-4,4'-diphenylmethane, barbituric acid and aminopropyl phenylsiloxane oligomer. *J. Taiwan Inst. Chem. Eng.* **2016**, *67*, 88–97. [[CrossRef](#)]
82. Yu, F.E.; Lee, H.Y.; Hsu, J.M.; Pan, J.P.; Wang, T.H.; Chen, Z.Y.; Chern, C.S. Effects of initial composition and temperature on the kinetics of polymerizations of N,N'-bismaleimide-4,4'-diphenylmethane with barbituric acid. *J. Taiwan Inst. Chem. Eng.* **2015**, *52*, 181–190. [[CrossRef](#)]
83. Pham, Q.T.; Hsu, J.M.; Wang, F.M.; Huang, X.C.; Tesemma, M.; Chern, C.S. Kinetics of nucleation-controlled polymerization of N,N'-bismaleimide-4,4'-diphenylmethane/barbituric acid. *Thermochim. Acta* **2016**, *641*, 1–7. [[CrossRef](#)]
84. MacNeil, D.D.; Dahn, J.R. Test of Reaction Kinetics Using Both Differential Scanning and Accelerating Rate Calorimetries As Applied to the Reaction of Li_xCoO_2 in Non-aqueous Electrolyte. *J. Phys. Chem. A* **2001**, *105*, 4430–4439. [[CrossRef](#)]
85. Pham, Q.T.; Hsu, J.M.; Wang, F.M.; Chen, M.P.; Chern, C.S. Isothermal polymerization kinetics of N,N'-bismaleimide-4,4'-diphenylmethane with cyanuric acid. *Thermochim. Acta* **2017**, *647*, 30–35. [[CrossRef](#)]
86. Pham, Q.T.; Zhan, Y.X.; Wang, F.M.; Chern, C.S. Mechanisms and kinetics of non-isothermal polymerization of N,N'-bismaleimide-4,4'-diphenylmethane with barbituric acid in dimethyl sulfoxide. *Thermochim. Acta* **2019**, *676*, 139–144. [[CrossRef](#)]
87. Wang, F.M.; Alemu, T.; Yeh, N.H.; Wang, X.C.; Lin, Y.W.; Hsu, C.C.; Chang, Y.J.; Liu, C.H.; Chuang, C.I.; Hsiao, L.H.; et al. Interface Interaction Behavior of Self-Terminated Oligomer Electrode Additives for a Ni-Rich Layer Cathode in Lithium-Ion Batteries: Voltage and Temperature Effects. *ACS Appl. Mater. Interfaces* **2019**, *11*, 39827–39840. [[CrossRef](#)] [[PubMed](#)]
88. Wu, Y.S.; Pham, Q.T.; Yang, C.C.; Chern, C.S.; Babulal, L.M.; Seenivasan, M.; Bruncklaus, G.; Placke, T.; Hwang, B.J.; Winter, M. Study of electrochemical performance and thermal property of $\text{LiNi}_0.5\text{Co}_0.2\text{Mn}_0.3\text{O}_2$ cathode materials coated with a novel oligomer additive for high-safety lithium-ion batteries. *Chem. Eng. J.* **2021**, *405*, 126727–126742. [[CrossRef](#)]
89. Pham, Q.T.; Chern, C.S. Applications of polymers in lithium-ion batteries with enhanced safety and cycle life. *J. Polymer Res.* **2022**, *29*, 124–151. [[CrossRef](#)]

Disclaimer/Publisher's Note: The statements, opinions and data contained in all publications are solely those of the individual author(s) and contributor(s) and not of MDPI and/or the editor(s). MDPI and/or the editor(s) disclaim responsibility for any injury to people or property resulting from any ideas, methods, instructions or products referred to in the content.